Title
Immunological consequences of ketogenic diet-induced shifts in the gut microbiota

Author
Ang, Qi Yan

Publication Date
2019

Peer reviewed|Thesis/dissertation

Immunological consequences of ketogenic diet-induced shifts in the gut microbiota

by
Qi Yan Ang

DISSERTATION
Submitted in partial satisfaction of the requirements for degree of
DOCTOR OF PHILOSOPHY

in

Biomedical Sciences

in the

GRADUATE DIVISION
of the
UNIVERSITY OF CALIFORNIA, SAN FRANCISCO

Approved:

DocuSigned by:
Allison Xu
82B559F23B4F486...

Allison Xu
Chair

DocuSigned by:
Peter Turnbaugh

Peter Turnbaugh

DocuSigned by:
K S Pollard

Katie Pollard

DocuSigned by:
Susan Lynch
1A38FCA893D34C5...

Susan Lynch

Committee Members

Dedicated to my family and Jeremy

Acknowledgements

I am grateful to my PhD supervisor, Dr. Peter James Turnbaugh, for being a fabulous mentor throughout my thesis research. Thank you for offering me a place as the first graduate student in your lab, and for providing me with invaluable feedback and guidance along my PhD journey. You have been a brilliant and supportive mentor. To quote Socrates, “Education is the kindling of a flame, not the filling of a vessel.” Your words of encouragement have inspired me with confidence in all that I have learned over the past five years, and, more importantly, with the desire to continue learning as I take the next steps on my scientific journey.

I would also like to thank the past and present members of the Turnbaugh lab. I’ve enjoyed working among this group of very happy, motivated, and incredibly talented scientists. To the postdocs in the lab: I have learned so much from each and every one of you — thank you for your generosity in sharing your knowledge and experience, even and especially when you had your own projects and deadlines to attend to. I am also grateful to the growing community of graduate students in the lab for the great company. I will certainly miss all the fun times with members in the lab, from Hoopy hours and birthday celebrations to spikeball at the beach and swimming practices with Kathy Lam and Maggie Alexander (who taught me flip turns).

Modern science is truly a team sport, and the success of my thesis work reflects the contributions of a variety of mentors with different academic backgrounds and specialties. A special shout-out to Maggie Alexander who brought immunology expertise to the lab and helped catalyze an exciting turn in my thesis project to study the impact of diet-induced gut microbial shifts on immune cells. Also to John Newman, who introduced

me to the world of ketogenic diets and ketone mimetics; to Andrew Patterson, who provided metabolomics expertise; and to my clinical collaborators, who provided valuable human samples. I would also like to thank my thesis committee — Drs. Allison Xu, Katherine Pollard and Susan Lynch — for their support and suggestions; the UCSF gnotobiotic core facility, where I performed many experiments with the help of the team led by Jessie Turnbaugh; and the Hooper staff, especially Ernesto Valencia and Daryll Gempis, who have gone above and beyond to make the Hooper a great place for research.

I would also like to acknowledge the support I have received from Singapore's national Agency for Science, Technology and Research (A*STAR). Without the scholarships and funding I've held throughout the last nine years, I would not have been able to pursue my undergraduate studies at the University of Cambridge nor my PhD studies here at UCSF. A*STAR's generous support afforded me the opportunity to attend some of the best institutions in the world and engendered in me a global outlook that I will carry forward in all that I do.

Outside of the lab, the unwavering support of my family and friends has been indispensable. I am grateful to my family for their constant love, support, and incredible patience while I pursue higher education overseas. I am deeply appreciative of the countless times you made your way across the world to visit me, despite the long travels and significant cost. Finally, I would like to thank Jeremy Markson for accompanying me on this PhD journey. Thank you for your interest in my work and constant moral support. Despite the stresses of being a PhD student, you have helped me lead a fun and colorful life outside of academic research and kept me sane and happy.

Contributions

My thesis work presented here is adapted from a manuscript in revision. Peter J. Turnbaugh supervised the entirety of this work. The multicenter human study described in Chapter 2 was designed and conducted by Kevin D. Hall, Rudolph L. Leibel, Eric Ravussin and Michael Rosenbaum. John C. Newman conducted the longevity mouse cohort described in Chapter 3 and designed the ketone ester in Chapter 4 under the guidance of Eric Verdin. Fecal metabolomic assays described in Chapters 2 and 4 were performed by Jingwei Cai under the guidance of Andrew D. Patterson. Margaret Alexander performed the flow cytometric analyses described in Chapter 5. I generated all other data described in this work.

Immunological consequences of ketogenic diet-induced shifts in the gut microbiota

Qi Yan Ang

Abstract

Very low-carbohydrate, high-fat “ketogenic” diets (KDs) induce a pronounced shift in metabolic fuel utilization that elevates circulating ketone bodies; however, the downstream consequences of these compounds for host-microbiome interactions remains unknown. My thesis work shows that KDs alter the human and mouse gut microbiota in a manner distinct from high-fat diets (HFDs). Metagenomic and metabolomic analyses of stool samples collected during an 8-week inpatient study revealed marked shifts in gut microbial community structure and function during the KD. Gradient diet experiments in mice confirmed the unique impact of KDs relative to HFDs with a reproducible depletion of *Bifidobacteria*. *In vitro* and *in vivo* experiments showed that ketone bodies directly inhibit bifidobacterial growth. Finally, mono-colonizations and human microbiome transplantations into germ-free mice revealed that the KD-associated gut microbiota reduces the levels of pro-inflammatory Th17 cells in the gut. Together, these results highlight the importance of trans-kingdom chemical dialogues for mediating the host response to dietary interventions.

Table of Contents

List of Figures

List of Tables

Chapter 1.
Introduction

1.1 The gut microbiome

The trillions of microorganisms within the gastrointestinal tract are collectively termed the gut microbiota. Recent studies have highlighted the dynamic and complex crosstalk that exists between the host and its microbial communities. We now know that the gut microbiota perform many essential functions for the host including nutrient extraction (Cani et al. 2019), defense against pathogen colonization (Pickard et al. 2017), and modulation of immune function (Rooks and Garrett 2016). Alterations in gut microbiota have also been linked to a variety of conditions including metabolic (Koeth et al. 2013; Turnbaugh et al. 2006; Thingholm et al. 2019) and inflammatory diseases (Frank et al. 2007; Scher et al. 2013) and even cognitive dysfunction (Olson et al. 2018; Sharon et al. 2019), while recent work has also highlighted how microbial drug metabolism can influence treatment efficacy (Lam, Alexander, and Turnbaugh 2019). In turn, the gut microbiota are influenced by multiple host and environmental factors, with host diet as a major factor shaping gut microbial composition and function (Carmody et al. 2015). A multitude of studies have explored the impact of macronutrient intake on community composition of the gut microbiota, with a high-fat diet (HFD) being the most often-studied dietary intervention (Turnbaugh et al. 2008).

1.2 Ketogenic diets and the gut microbiome

Very low-carbohydrate, high-fat "ketogenic" diets (KDs) have become increasingly popular for weight loss and glycemic control, but the metabolic consequences of such diets are incompletely understood (Hall and Chung 2018). Given the emerging evidence that the gut microbiota is both highly sensitive to dietary intake (Carmody et al. 2015) and plays a central role in coordinating host energy balance (Bäckhed et al. 2004; Turnbaugh et al. 2006; Cani et al. 2019), I hypothesized that KDs could act in part by shaping the gut microbiota. The premise for this hypothesis is supported by multiple recent studies in rodent models demonstrating that the consumption of a KD alters the structure and function of the gut microbiota (Olson et al. 2018; Cani et al. 2007). This effect also appears to be relevant to the human gut microbiome in states of health and disease. For example, the consumption of a nearly carbohydrate-free KD derived entirely of animal products reproducibly altered the structure, gene expression, and metabolic activity of the human gut microbiome within days (David et al. 2014). Furthermore, the administration of a KD to non-alcoholic fatty liver patients altered the human gut microbiome (Mardinoglu et al. 2018).

Yet multiple fundamental questions remain unaddressed. The results of past human studies have been confounded by other changes in caloric and macronutrient intake (David et al. 2014; Mardinoglu et al. 2018) that could have ketogenesis-independent effects on the gut microbiome. More importantly, the mechanisms through which KDs alter gut bacterial abundance are currently unknown, as are the downstream consequences of these changes for host metabolic and immunologic phenotypes.

In my thesis work, I begin to address these questions through the combined use of controlled dietary interventions in overweight and obese individuals and follow-on studies in conventional and gnotobiotic mice. I show that the impact of KDs on the gut microbiota is distinctive from -- and in some cases the opposite of -- the impact of common high-fat, high-sugar “Western” diets. The observed changes in gut microbiota appear to be driven not only by dietary macronutrients but also by host production of ketone bodies, which inhibit bacterial growth in mice and *in vitro* mono-cultures. Ketogenesis reproducibly decreased the relative abundance of *Bifidobacteria* in humans and mice, which play a causal role in KD-associated decreases in intestinal inflammation. Together, these results emphasize the importance of considering the chemical dialogues between host and microbial cells to gain a more comprehensive view of the mechanistic links between diet and host physiology.

Chapter 2.

Ketogenic diets reproducibly alter the human gut microbiome

To study the impact of severe carbohydrate restriction on the human gut microbiota, I turned to fecal samples collected from an inpatient crossover study led by Kevin D. Hall (Hall et al. 2016). In this clinical study, 17 adult, overweight or class I obese, non-diabetic male participants were first fed a baseline diet for 4 weeks (BD, 50% Carbohydrate, 15% Protein, 35% Fat) followed by a 4-week very-low-carbohydrate ketogenic diet (KD, 5% Carbohydrate, 15% Protein, 80% Fat)[1] **(Figure 2.1A)** which resulted in significant elevations in circulating plasma ketones, a hallmark of ketogenic diets **(Figure 2.1B)**. Diets provided were isocaloric during BD and KD periods and matched to each participant's energy expenditure. Five daily stool samples were collected in the final week of each diet period. As previously reported, the subjects were in a similar state of mild negative energy balance during the BD and KD fecal collection periods (Hall et al. 2016).

16S rRNA gene sequencing revealed that the KD resulted in significant compositional shifts of the gut microbiome across all individuals **(Figure 2.1C)** and altered the relative abundance of the major bacterial phyla **(Figure 2.1D)**, consistent with a prior human study from our lab (David et al. 2014). Nineteen genera were significantly altered with *Bifidobacterium* showing the greatest decrease on KD **(Figure 2.1E)**. Metagenomic shotgun sequencing of paired stool samples from the two diet arms confirmed the

[1] More details on the daily diet composition as well as sample menus during BD and KD diet stages can be found in Hall, Kevin D., Kong Y. Chen, Juen Guo, Yan Y. Lam, Rudolph L. Leibel, Laurel Es Mayer, Marc L. Reitman, et al. 2016. "Energy Expenditure and Body Composition Changes after an Isocaloric Ketogenic Diet in Overweight and Obese Men." *The American Journal of Clinical Nutrition* 104 (2): 324–33.

dramatic reduction of several bifidobacterial species on KD across all individuals **(Figures 2.2A and 2.2B)**. Global profiling of the fecal metabolome by ^{1}H NMR **(Figure 2.1F)** revealed distinct clustering between BD and KD diets despite no significant difference in bacterial load **(Figure 2.1G)** between stool samples from the two diet arms. Overall, these results suggest that KD reproducibly alters the human gut microbial community structure and function.

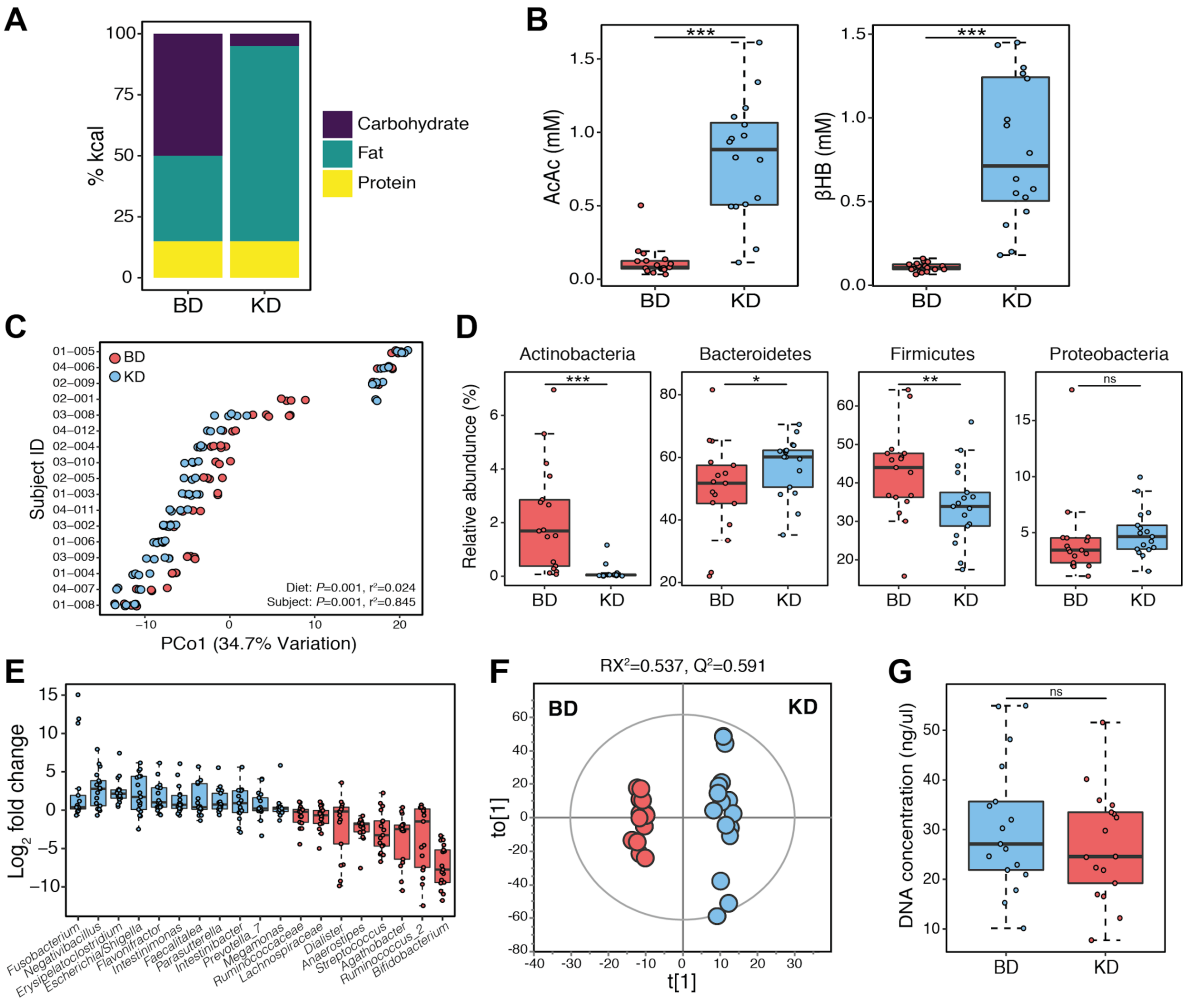

Figure 2.1. A ketogenic diet alters the human gut microbial community structure relative to an isocaloric control diet.

(A) Daily diet composition during the baseline diet (BD) and ketogenic diet (KD) stages respectively, represented in percent calories. (B) Plasma levels of the ketone bodies acetoacetate (AcAc) and β-hydroxybutyrate (βHB) significantly increased during KD across all 17 study participants (***$P < 0.001$; paired *t*-test). (C) Reproducible shifts in gut microbial community structure are observed across study participants on the first principle coordinate (PCo1) of PhILR Euclidean distances between the two diet stages ($P = 0.001$, $r^2 = 0.024$, ADONIS with Subject ID as stratum), despite significant inter-individual variation in community structure between subjects ($P = 0.001$, $r^2 = 0.845$, ADONIS testing for Subject ID). (D) KD alters the relative abundance of the major phyla in the human gut microbiota (*$P < 0.05$, **$P < 0.01$, ***P < 0.001, ns = not significant; paired Wilcoxon test). (E) Fold change of genera whose abundances were significantly altered by KD (FDR < 0.05, DESeq2). (F) OPLS-DA score plot from ^{1}H NMR spectra of fecal metabolite profiles between BD and KD diet stages across 17 study participants. The OPLS-DA model was validated with a 7-fold cross validation method; R^2 value represents predictive power (R^2>0.5 suggests model is robust) and Q^2>0.4 value suggests the model is valid. (G) Fecal DNA content is not significantly different between the two diet stages (ns, not significant; paired *t*-test). Data are presented as mean±SEM.

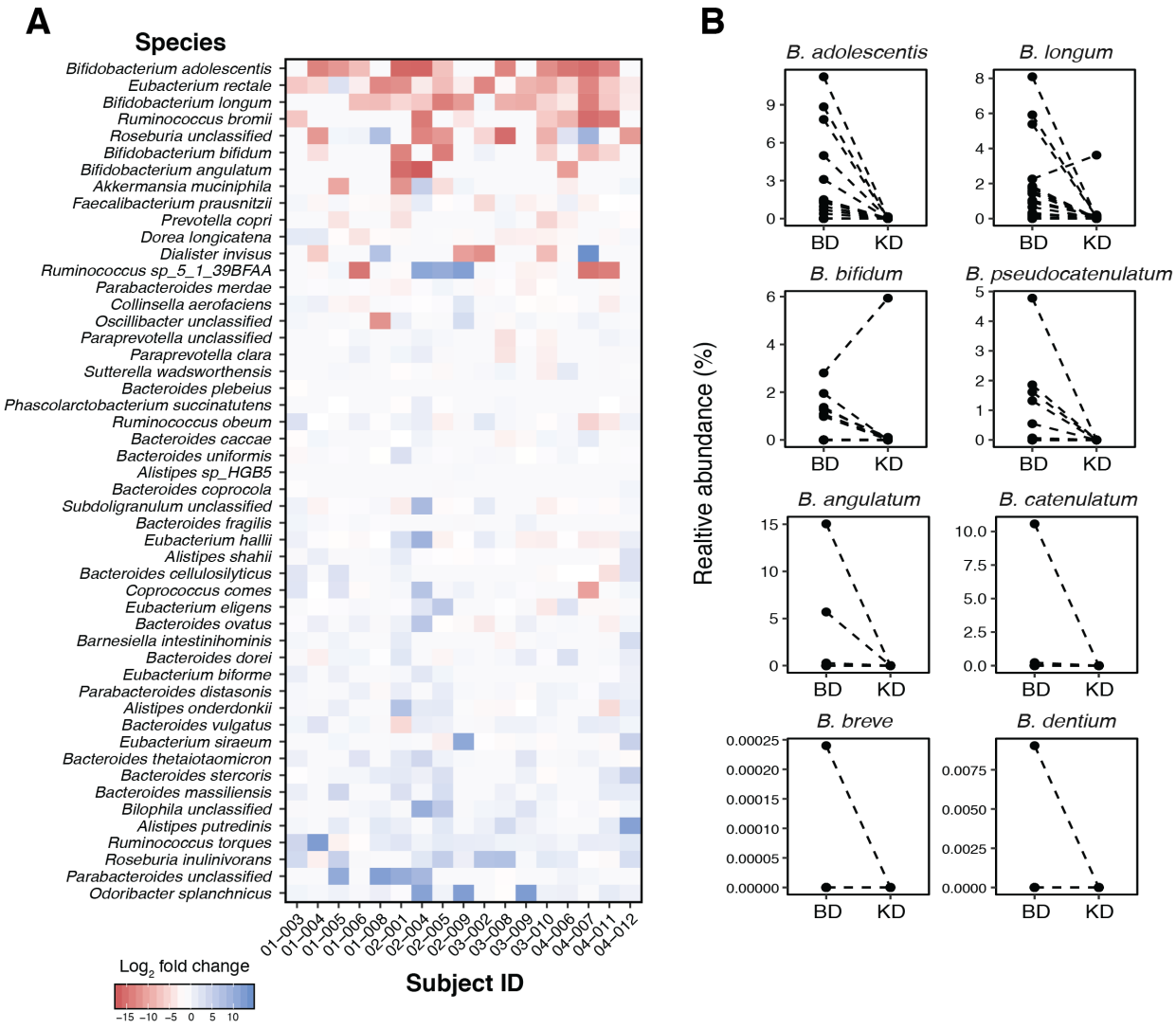

Figure 2.2. Metagenomic sequencing reveals decreased abundance of bifidobacterial species on the ketogenic diet in our human cohort.
(A) Heatmap showing fold change of the 50 most abundant species, comparing the ketogenic diet (KD) to baseline diet (BD) stages across all 17 subjects in our human study. Bacterial species are ordered by the magnitude and direction of the average fold change, from the most negative (top) to positive (bottom). (B) The ketogenic diet results in consistent reductions in the abundance of bifidobacterial species in our human cohort. Each line connects paired samples between the two diet arms from each study subject, for bifidobacterial species detected in a study subject's gut microbiota.

Chapter 3.

Ketogenic diets alter the gut microbiome in a manner distinct from high-fat diets

3.1 Short and long-term diet experiments

An apparent paradox is that while studies in mice have repeatedly found that high-fat, high-sugar (HFHS) diets increase the *Firmicutes* at the expense of the *Bacteroidetes* (Carmody et al. 2015; Turnbaugh et al. 2008; Bisanz et al. 2019), my results in humans demonstrate that high-fat, very low-carbohydrate KDs have the inverse effect. To address this discrepancy, I fed conventionally-raised C57BL/6J adult mice three semi-purified diets with identical ingredients but varying in the proportion of calories from fat and carbohydrates **(Figure 3.1A)**: low-fat diet (LFD, 78/12/10 carbohydrates/fat/protein); high-fat diet (HFD, 15/75/10); and KD (0/90/10). As expected, the KD significantly raised plasma levels of the ketone body β-hydroxybutyrate (βHB) compared to baseline levels in the other diet groups **(Figure 3.1B)**. Due to the relatively high caloric density of HFD and KD, mice fed these diets ate more calories on average compared to mice fed chow or LFD, with no difference in caloric intake observed between the HFD and KD diet groups **(Figure 3.1C)**. There was a significant effect of diet on gut microbial composition **(Figure 3.1D).** Consistent with prior work in mice and humans (Carmody et al. 2015; David et al. 2014), the HFD significantly increased the relative abundance of the *Firmicutes* phylum at the expense of the *Bacteroidetes*; however, the KD partially reversed this trend **(Figure 3.1E)**. I also observed that the KD significantly decreased the relative abundance of *Actinobacteria* to a level similar to that of a low-fat, high-plant-polysaccharide chow diet

(Figure 3.1E). Comparing HFD and KD, there were ten significantly altered genera **(Figure 3.1F)** with *Bifidobacterium* showing one of the greatest decreases on KD similar to that observed in the human study **(Figure 2.1E)**. To address the possibility that overall alterations in microbial abundance could underpin the observed changes in microbial compositionality (Vandeputte et al. 2017), I determined total microbial colonization level by quantitative PCR (qPCR); there was no significant difference in microbial load among the diets (**Figure 3.1G**). Furthermore, these observed microbial shifts were stable and reproducible over 10 weeks of dietary intervention **(Figures 3.2A and 3.2B)** in animals at an independent mouse facility and also with even longer-term feeding of these diets in a healthspan and longevity cohort (Newman et al. 2017) where I collected fecal samples from mice fed these respective diets over a period of up to 11 months at the time of sampling **(Figures 3.2C and 3.2D).**

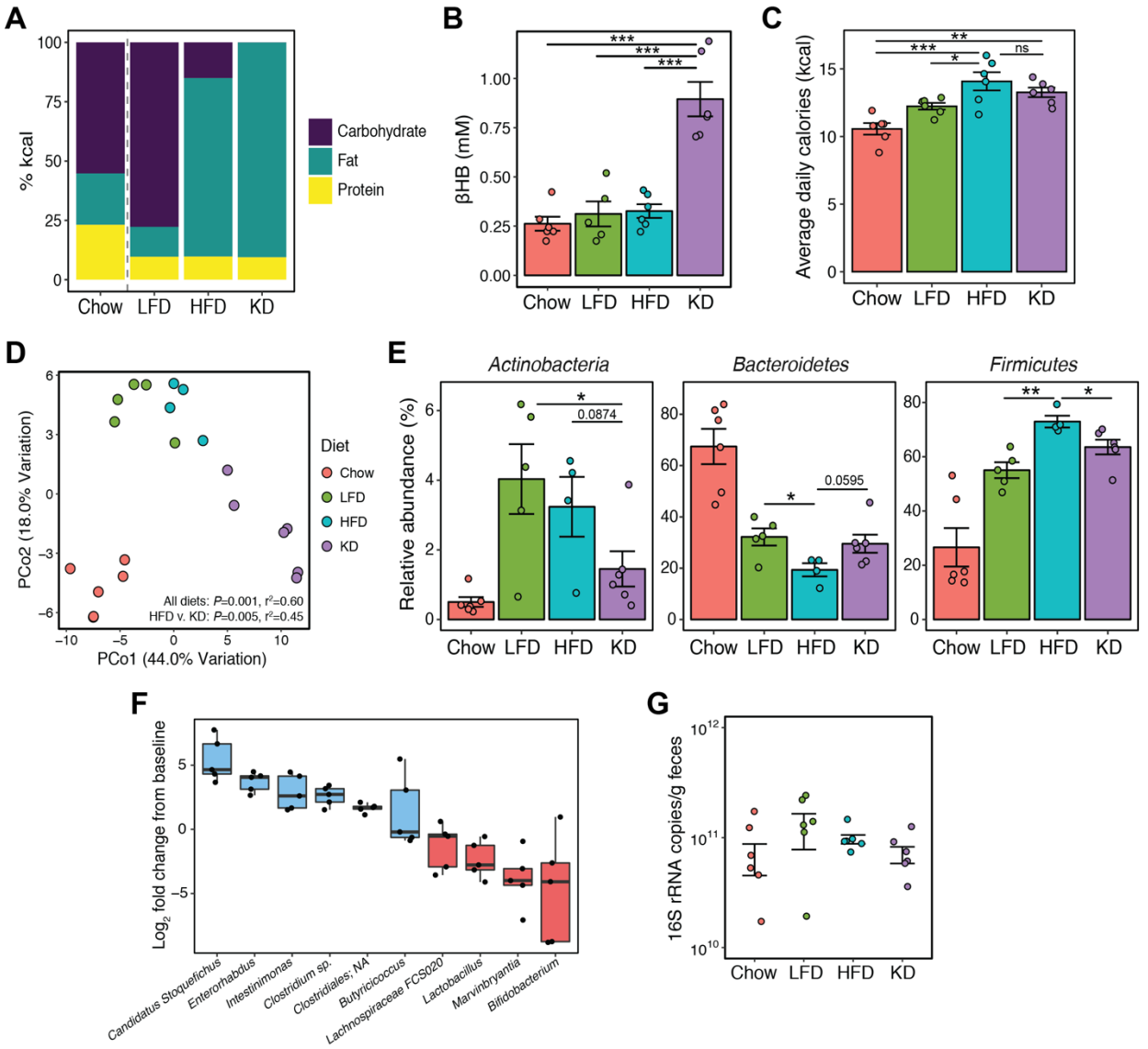

Figure 3.1. The impact of a ketogenic diet on the gut microbiota is distinct from a high-fat diet.

(A) Macronutrient composition (in percent calories) of the chow diet and three semi-purified diets: low-fat diet (LFD), high-fat diet (HFD) and ketogenic diet (KD). (B) Circulating β-hydroxybutyrate (βHB) levels in mice on diets for 3 weeks (n = 6 mice/group, ***P < 0.001; one-way ANOVA with Tukey's test). (C) Average daily calorie intake in mice fed the respective diets over three weeks (n = 6 mice/group, *P < 0.05, **P < 0.01, ***P < 0.001, ns = not significant; one-way ANOVA with Tukey's test). (D) Principal coordinate analysis of PhILR Euclidean distances reveal significant effect of diet on community composition (P = 0.001, r^2 = 0.60; ADONIS) and also significant differences in community composition comparing HFD to KD (P = 0.005, r^2 = 0.45; ADONIS). (E) Relative abundance of the major phyla in the microbial communities of mice on respective diets (n = 4-6 mice/group, *P < 0.05, **P < 0.01; Kruskal-Wallis with Dunn's test). (F) Fold change from baseline of genera whose abundances were significantly different between HFD and

KD (FDR < 0.1, DESeq2), in mice fed KD (n = 6 mice). (G) Fecal bacterial DNA content, expressed as 16S rRNA gene copies/ gram wet weight, of mice on respective diets is not significantly different (n = 6 mice/group; one-way ANOVA with Tukey's test). Data are presented as mean±SEM. Each data point represents an individual, singly-housed animal.

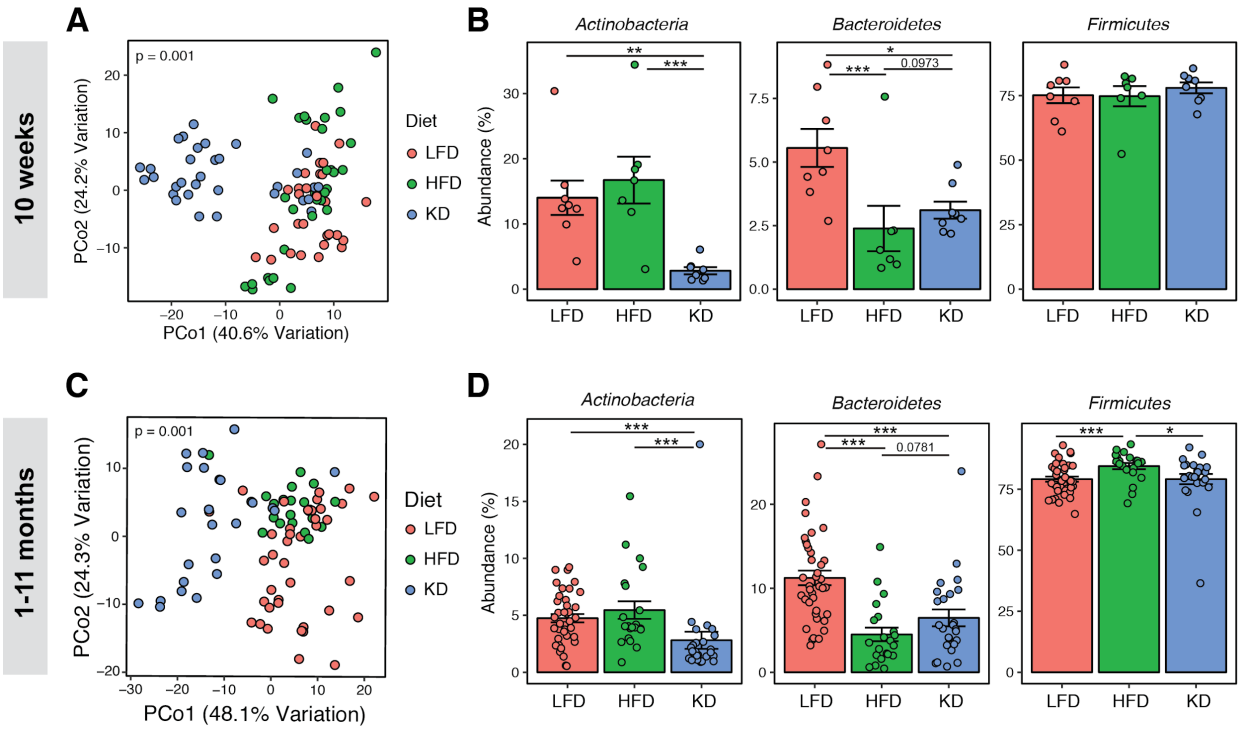

Figure 3.2. The ketogenic diet results in stable and reproducible shifts in gut microbial composition.
(A) Principal coordinate analysis of PhILR Euclidean distances reveal distinct clustering of KD samples and a significant effect of diet on community composition (P = 0.001, r^2= 0.31, ADONIS) in mice fed the respective diets over 10 weeks. (B) Relative abundance of the major phyla in the microbial communities of mice on respective diets, averaged from weekly samples. (n = 8 mice/group with mice housed in pairs, *P < 0.05, **P < 0.01, ***P < 0.001; Kruskal-Wallis with Dunn's test). (C) Principal coordinate analysis of fecal samples collected at a single time point from a healthspan and longevity cohort (Newman et al. 2017) reveals a significant effect of diet on community composition (P = 0.001, r^2= 0.33, ADONIS) with long-term feeding of the respective diets (range 28 - 311 days at the time of sample collection). Each data point represents an individual animal (n = 21 - 35 mice/group with 3-5 mice housed per cage). (D) Relative abundance of the major phyla in the microbial communities of mice fed the respective diets long-term (n = 21 - 35 mice/group, *P < 0.05, ***P < 0.01; Kruskal-Wallis with Dunn's test). Data are presented as mean±SEM.

3.2 Diet experiments using an alternative carbohydrate source

Next, I sought to determine if the effect of a KD on the gut microbiota would be replicable with an alternative carbohydrate source enriched for plant polysaccharides that require gut microbial metabolism for their digestion. I designed a parallel set of semi-purified diets varying in carbohydrate and fat content and using the same ingredients except replacing half of the corn starch by weight with a resistant starch source (high amylose corn starch) **(Figure 3.3A)**. I then performed an experiment in which mice were sequentially fed these diets in order of decreasing dietary carbohydrate content, switching to a different diet every 3 days. Consistent with prior work in mice and humans documenting the rapid effect of diet on the gut microbiota (David et al. 2014; Carmody et al. 2015; Turnbaugh et al. 2009), I observed rapid shifts in the gut microbial communities of mice within a day of feeding on each diet **(Figure 3.3B)**. I also observed that the addition of resistant starch to the semi-purified diets preserved the relative abundance of *Bacteroidetes* relative to the chow diet and the proportion of *Bacteroidetes* decreased while *Firmicutes* increased almost linearly with decreasing dietary carbohydrate content **(Figure 3.3C)** revealing a dose-dependent response to diet as previous work suggested (Carmody et al. 2015). In contrast to the two major bacterial phyla, *Actinobacteria* showed a non-linear dose response to dietary carbohydrate content which was also detectable at the genus level (*Bifidobacterium*) **(Figure 3.3D)**, a result confirmed with a 3-week dietary intervention where mice were split into separate diet groups **(Figure 3.3E)**, and comparable to that observed in the original diet experiments I performed using diets without added resistant starch **(Figure 3.1E)**. To my knowledge, this is the first example of a non-linear dose response between a dietary perturbation and the gut microbiome, suggesting that there

may be a “tipping point” at which the host and/or the microbiome responds differently to macronutrient intake.

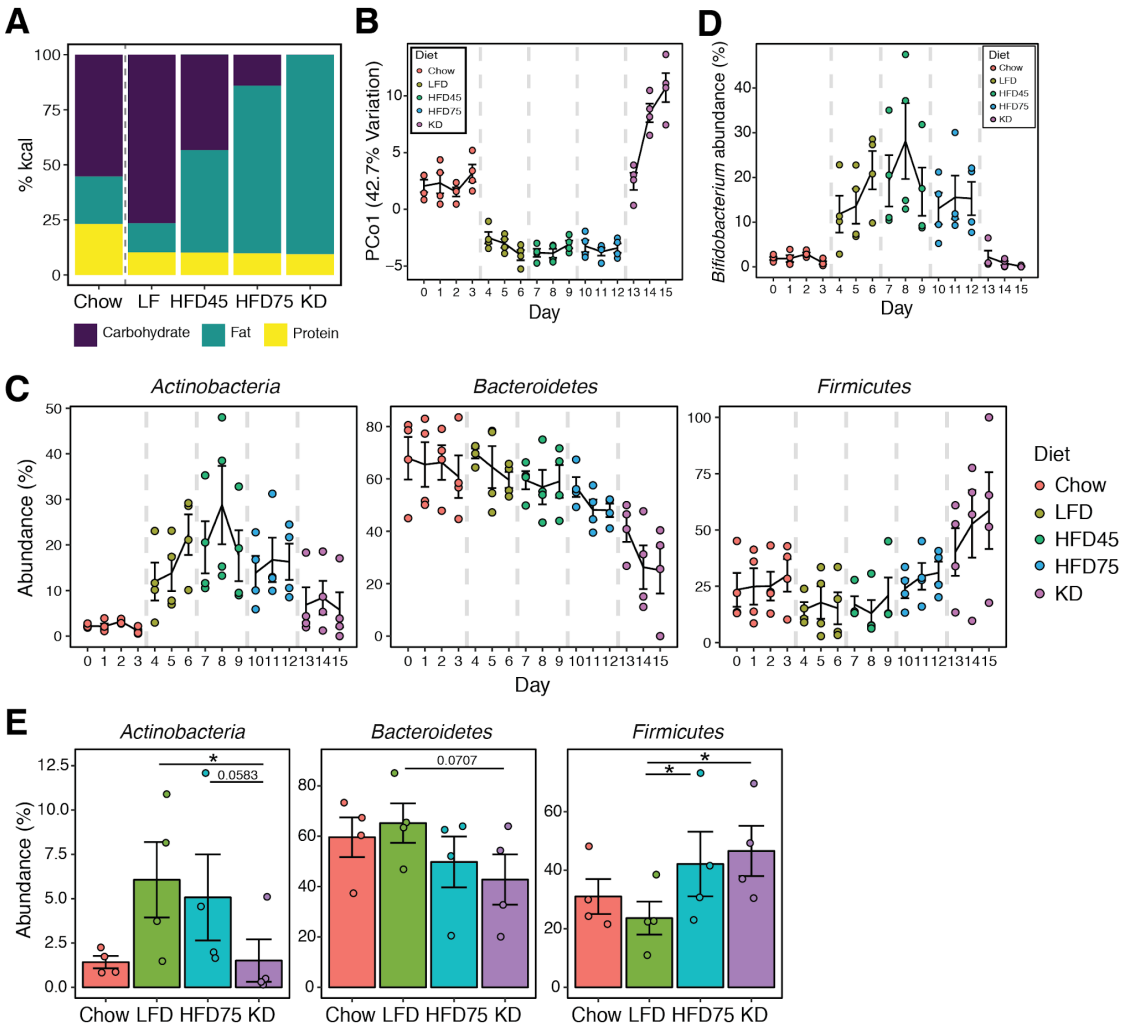

Figure 3.3. The effect of a ketogenic diet on the gut microbiota is replicable with an alternative carbohydrate source enriched for plant polysaccharides.
(A) Macronutrient composition (in percent calories) of standard chow and a series of semi-purified diets containing resistant starch and with varying carbohydrate and fat content: low-fat diet (LFD), 45%-fat high-fat diet (HFD45), 75%-fat high-fat diet (HFD75), and ketogenic diet (KD). (B) Rapid shifts in gut microbial composition are observed within a day of feeding of each diet. Mice were fed each diet for 3 days in a sequential order: Chow → LFD → HFD45 → HFD75 → KD, and dashed vertical lines represent the switch of diets. Axis 1 of principal coordinate analysis (PCo1) on PhILR Euclidean distances is shown over the 15-day study period (n = 4 mice). (C) Relative abundance of the major phyla in the microbial communities of mice fed the respective diets over 15 days reveal both linear (*Bacteroidetes* and *Firmicutes*) and non-linear (*Actinobacteria*) dose responses to dietary carbohydrate (n = 4 mice). (D) Abundance of *Bifidobacterium* in the murine fecal microbiota over study period, showing decrease on KD to a level similar to that of chow diet (n = 4 mice). (E) Relative abundance of the major phyla in the microbial communities of mice fed the respective diets over 3 weeks in a separate experiment (n = 4 mice/group, $*P < 0.05$; Kruskal-Wallis with Dunn's test). Data are presented as mean±SEM. Each data point represents an individual, singly-housed animal.

3.3 Fine dietary gradient experiments

I then sought to more precisely identify the tipping point at which the gut microbiota responds differently to changes in the proportions of dietary macronutrients. I designed additional diets containing varying carbohydrate (CHO) content that were between the original HFD (HFD75; 15% CHO) and KD (0% CHO) **(Figure 3.4A)**: HFD85 (5/85/10 CHO/fat/protein) and HFD89 (1/89/10). HFD75 (15% CHO) was based on a previous study (Newman et al. 2017) which determined the lowest possible dietary carbohydrate content that would not increase circulating ketone bodies over background levels. Mice fed the diets containing less than 15% carbohydrate (HFD85, HFD89, KD) exhibited elevated ketone body levels over baseline levels in mice fed HFD75, with circulating ketone body levels increasing as dietary carbohydrate content decreased **(Figure 3.4B)**. Despite these relatively modest changes in macronutrient composition, I observed broad changes in gut microbial composition at the phylum level, with a significant increase in the abundance of *Bacteroidetes* on all three diets compared to HFD75 and a progressive decrease in *Actinobacterial* abundance with decreasing carbohydrate content **(Figure 3.4C)**. These results suggest that partial induction of ketogenesis is sufficient to alter the gut microbiota despite the continued intake of carbohydrates.

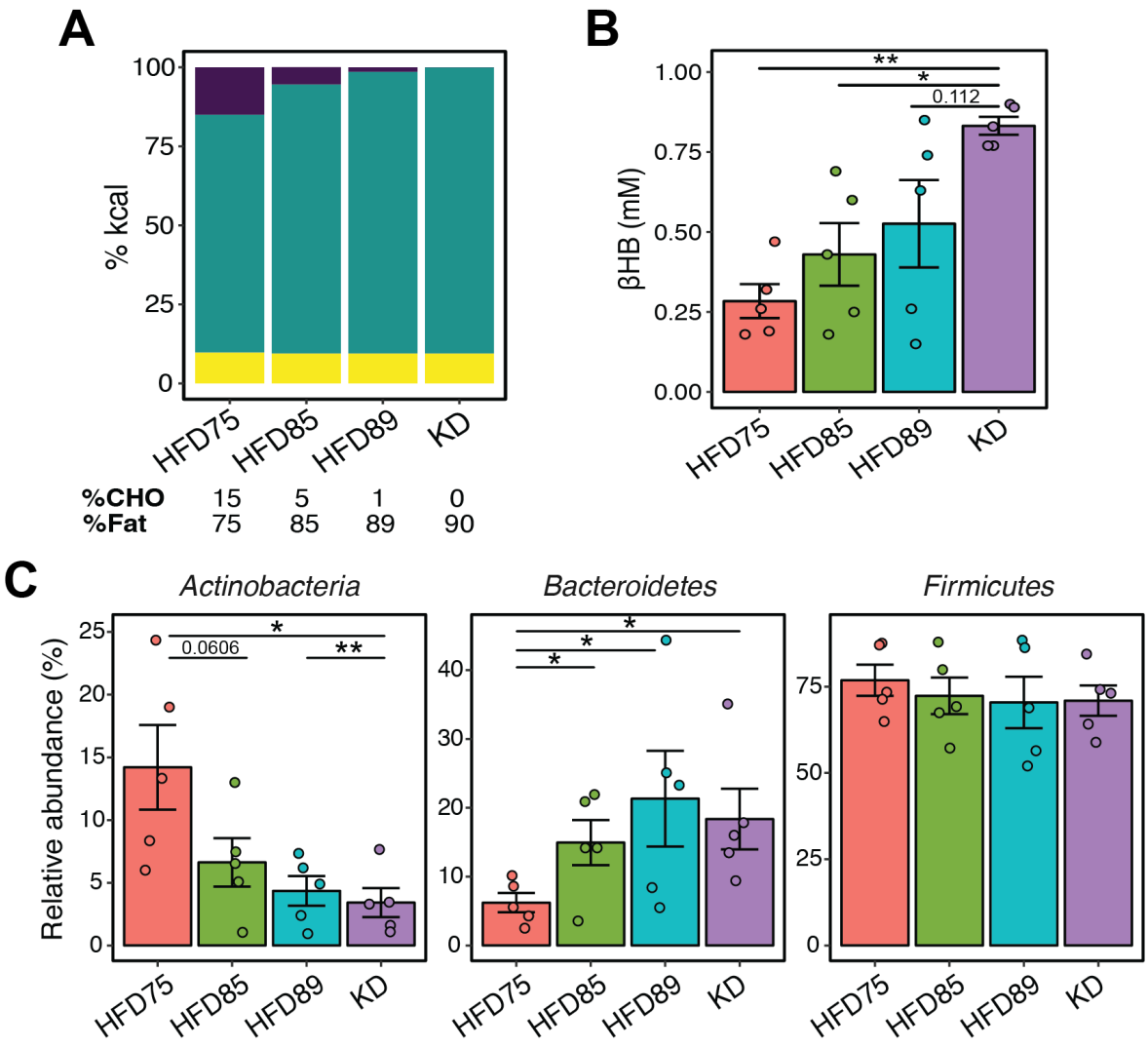

Figure 3.4. Modest changes in dietary carbohydrate associated with partial ketogenesis is sufficient to alter gut microbial composition.
(A) Macronutrient composition (in percent calories) of four semi-purified diets in order of decreasing carbohydrate content from 15% (HFD75) to 0% (KD). The carbohydrate (CHO) and fat content of each diet are shown below the barplots, with protein content matched across all diets. (B) Circulating β-hydroxybutyrate (βHB) levels in mice fed diets shown in panel G for 3 weeks (n = 5 mice/group, *$P < 0.05$, **$P < 0.01$; one-way ANOVA with Tukey's test). (C) Relative abundance of the major phyla in the microbial communities of mice on respective diets (*$P < 0.05$, **$P < 0.01$; Kruskal-Wallis with Dunn's test). Data are presented as mean±SEM. Each data point represents an individual, singly-housed animal.

Chapter 4.

Mechanistic links between the ketogenic diet and gut microbiome

4.1 Mucus foraging

I next wanted to explore the potential mechanism(s) that could contribute to the gut microbial changes between the HFD and KD. I first considered the contribution of the mucus layer, given previous work which demonstrated the promotion of mucus foraging activity in the gut bacteria of mice fed polysaccharide-deficient diets (Earle et al. 2015; Desai et al. 2016; Sonnenburg et al. 2005). Since carbohydrates in particular dietary fiber or complex carbohydrates that reach the distal gut are the principal carbon and energy source for colonic microbes, I wondered if the lack of dietary carbohydrates on KD could be driving the gut microbial response to KD. Previous reports have shown that low-fiber diets promote the expansion and activity of colonic mucus-degrading bacteria which utilize host-secreted mucus glycoproteins as an alternative nutrient source, correlating with reduced thickness of the mucus layer in gnotobiotic and humanized mouse models (Earle et al. 2015; Desai et al. 2016). However, quantification of the overall mucus thickness on methacarn-fixed distal colon sections did not reveal thinning of the mucus layer on KD **(Figures 4.1A, 4.1B)**, suggesting that KD maintains a robust mucus layer in conventional mice despite lack of fermentable carbohydrates. I also did not observe changes in the mRNA expression of mucin-2 glycoprotein (MUC2), the main colonic mucin isoform, thus ruling out compensatory changes in MUC2 gene expression in the host epithelium **(Figure 4.1C)**. Furthermore, MUC2-deficient mice fed KD exhibit changes

in the gut microbiota similar to that of wild-type mice **(Figure 4.2)**, suggesting that the presence of colonic mucins is not necessary for the observed gut microbial changes on KD. Overall, these results suggest that mucus-degrading activity is unlikely to be a significant driver of the gut microbial shifts between HFD and KD.

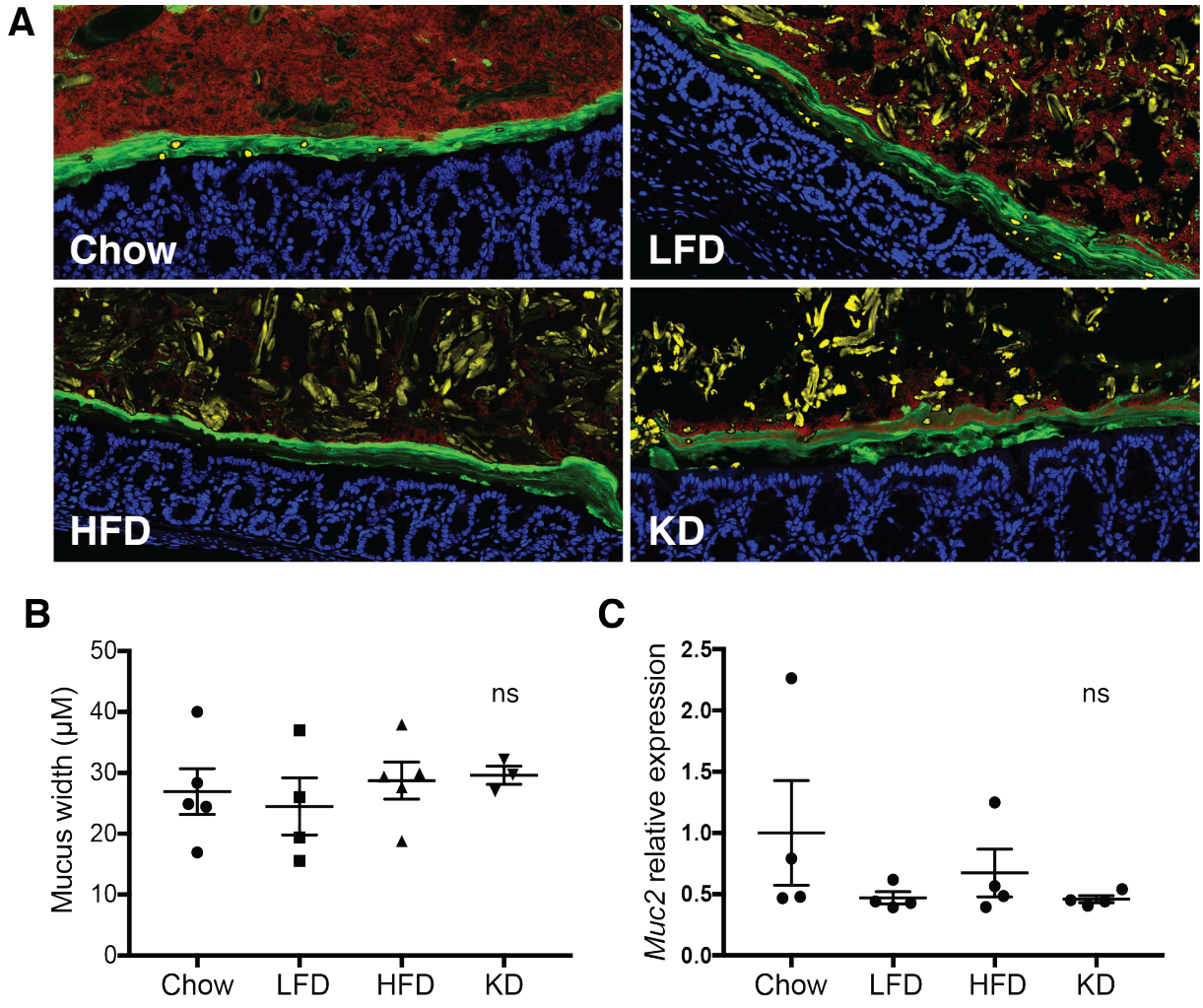

Figure 4.1. A ketogenic diet maintains a robust mucus layer despite lack of fermentable carbohydrates.
(A) Representative images of distal colon sections from conventional mice fed chow, low-fat diet (LFD), high-fat diet (HFD), or ketogenic diet (KD). Sections were stained with DAPI (epithelium, blue), UEA1 lectin (mucus, green) and EUB338 universal bacterial FISH probe (red). Images were further processed using BacSpace (Earle et al. 2015) and the computed luminal debris appears in yellow. (B) Average mucus widths in distal colons of conventional mice fed the respective diets after 3 weeks, quantified using BacSpace (Earle et al. 2015) (n = 3 - 5 mice/group, ns = not significant; one-way ANOVA). (C) Quantitative PCR of colonic *Muc2* transcripts reveal no significant difference in *Muc2* relative gene expression (n = 3 - 5 mice/group, ns = not significant; one-way ANOVA). Data are presented as mean±SEM. Each data point represents an individual, singly-housed animal.

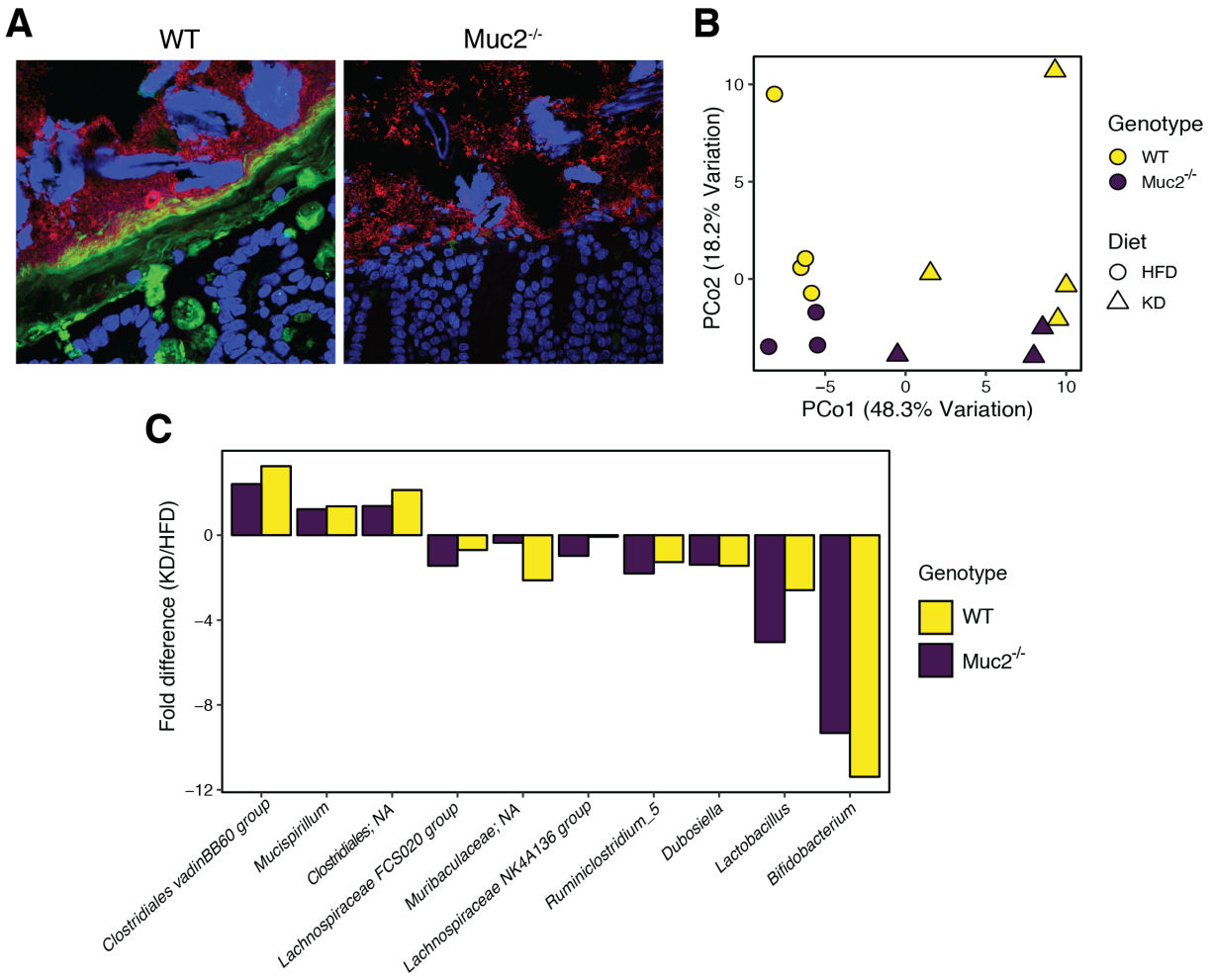

Figure 4.2. Gut microbial shift on a ketogenic diet is independent of colonic mucin. (A) Representative images of distal colon sections from wild-type (WT) and Muc2$^{-/-}$ mice respectively, showing lack of goblet cells and mucus layer in Muc2$^{-/-}$ mice with bacteria in close contact with gut epithelium. Sections were stained with DAPI (epithelium, blue), UEA1 lectin (mucus, green) and EUB338 universal bacterial FISH probe (red). (B) Principal coordinate analysis of PhILR Euclidean distances reveal significant clustering of microbial communities in WT and Muc2$^{-/-}$ littermates by diet (P = 0.001, r^2= 0.41, ADONIS) but not genotype (P = 0.076, r^2= 0.096, ADONIS); n = 3-4 mice per genotype-diet group. (C) Fold difference of genera whose abundances are significantly different between HFD and KD (FDR < 0.1, DESeq2), in WT and Muc2$^{-/-}$ mice respectively (n = 3-4 mice per genotype-diet group).

4.2 Bile acids

I next considered bile acids as another potential mechanism due to their role in fat emulsification; however, there was no significant difference in the overall bile acid pool in the human fecal samples comparing BD to KD **(Figure 4.3A)** nor in mouse cecal contents collected on the HFD or KD **(Figure 4.3B)**. Five bile acid species were found to be significantly different between the two diet arms in the human study: decreased levels of ursocholanic acid and lithocholic acid, and increased levels of deoxycholic acid, β-muricholic acid and taurolithocholic acid on the KD relative to BD. However, none of these changes were recapitulated in the mouse model thus ruling out differences in bile acids as a common factor driving the gut microbial changes observed on the ketogenic diet in mice and humans.

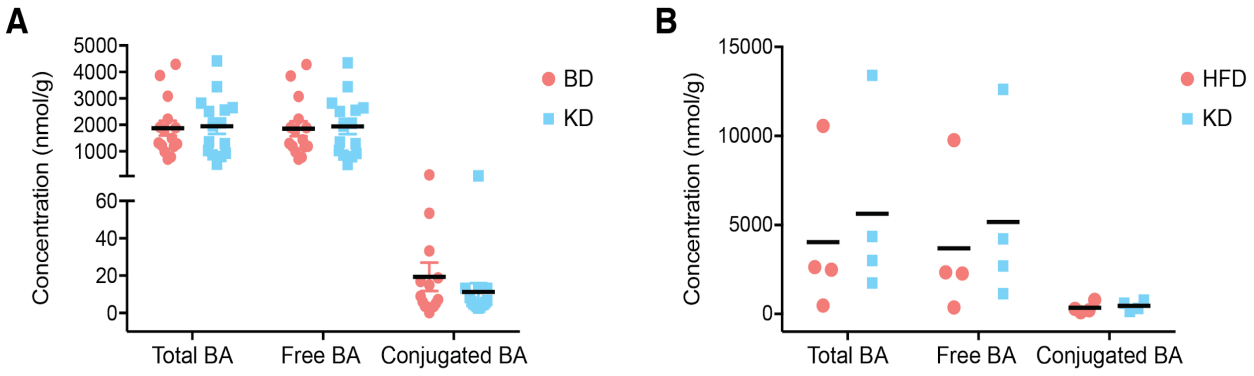

Figure 4.3. Overall bile acid pool is not significantly altered by a ketogenic diet in humans and mice.
(A, B) Concentration of total, free, and conjugated bile acids (BA) is not significantly different in (A) fecal samples from study participants during the baseline diet (BD) and ketogenic (KD) diet stages, nor (B) cecal contents from mice fed a high-fat diet (HFD) or ketogenic diet (KD). Data points represent paired stool samples from study participants during the two diet arms (A) or individual mice (B). Statistical analyses were performed using paired (A) or unpaired (B) *t* tests.

4.3 Ketone bodies

A far less well-characterized factor that could in theory impact gut bacterial growth is the ketone bodies that are significantly elevated on the KD compared to the HFD in human and mouse studies **(Figure 2.1B, 3.1B, and 3.4B)**, which are indicative of increased lipid oxidation in response to severe carbohydrate restriction. Interestingly, while the liver is the primary ketogenic organ in mammals, gut epithelial cells are also capable of producing ketone bodies (Puchalska and Crawford 2017), and previous work has shown increased local concentrations of βHB in the intestines with KD feeding (Tognini et al. 2017). This prompted me to wonder if production of ketone bodies by the gut epithelium during KD might impact the gut microbiome.

To investigate the impact of ketone bodies on the gut microbiome in the absence of carbohydrate restriction, I supplemented the HFD and KD with a synthetic ketone ester (KE) compound **(Figure 4.4A)** that is readily hydrolyzed in the intestinal lumen to produce β-hydroxybutyrate (βHB), thus mimicking intestinal production of ketone bodies. Given the nature of βHB as an organic acid that is rapidly catabolized, the use of this ketone ester as a prodrug avoids the problem of excessive acid or salt load with exogenous delivery βHB while sustaining βHB levels over a long period (Newman and Verdin 2017). The ketone ester consists of three constituent groups linked by ester bonds: the ketone body βHB, hexanoic acid (6-carbon fatty acid), and hexanol (6-carbon alcohol); the ester bonds are readily cleaved by esterases ubiquitous in the gut releasing free βHB as well as hexanol and hexanoic acid which are transported to the liver where they are further metabolized to βHB. In two independent experiments, I showed that supplementation of the ketone ester to a HFD (HFD-KE diet) significantly raised circulating levels of βHB over

baseline on the HFD, albeit at comparative smaller magnitude than KD consumption over 3 weeks **(Figure 4.4B)**. More importantly, I also showed that dietary KE supplementation increased βHB levels in the intestinal lumen **(Figure 4.4C)**, providing evidence that the KE compound could successfully reach the intestinal lumen and is hydrolyzed locally to release βHB, thus allowing me to investigate how the ketone body could potentially interact with gut bacteria. To my knowledge, there is currently no published data demonstrating the local regulation of βHB in the gut with dietary supplementation of ketone esters in rodent models nor humans, which highlights the practical implications of this work given the growing interest in the use of exogenous ketone bodies as potential therapeutic tools (Murray et al. 2016; Stubbs et al. 2017; Veech et al. 2017; Clarke et al. 2012).

I profiled the gut microbial communities of mice fed the respective diets via 16S rRNA gene sequencing, revealing that KE supplementation significantly altered gut microbial composition **(Figure 4.4D)**. Next, I sought to identify bacterial taxa that were specifically altered by the presence of βHB and would therefore exhibit changes in abundance with a similar pattern to the expected levels of βHB in the gut lumen. I searched for genera that were consistently altered in comparisons between the HFD and KD in addition to KE supplementation, revealing three genera that overlapped in directionality of fold change which were *Bifidobacterium*, *Lactobacillus,* and *Acetatifactor* **(Figure 4.4E)**. In particular, *Bifidobacterium* exhibited changes in abundances that were commensurate with βHB levels in mice fed HFD, KD or ketone-supplemented diets **(Figure 4.4E)**, consistent with my observations that *Bifidobacterium* showed decreased

abundance on the KD in both humans and mice **(Figure 2.1E and 3.1F)**, suggesting that βHB can directly impact *Bifidobacterium* growth *in vivo*.

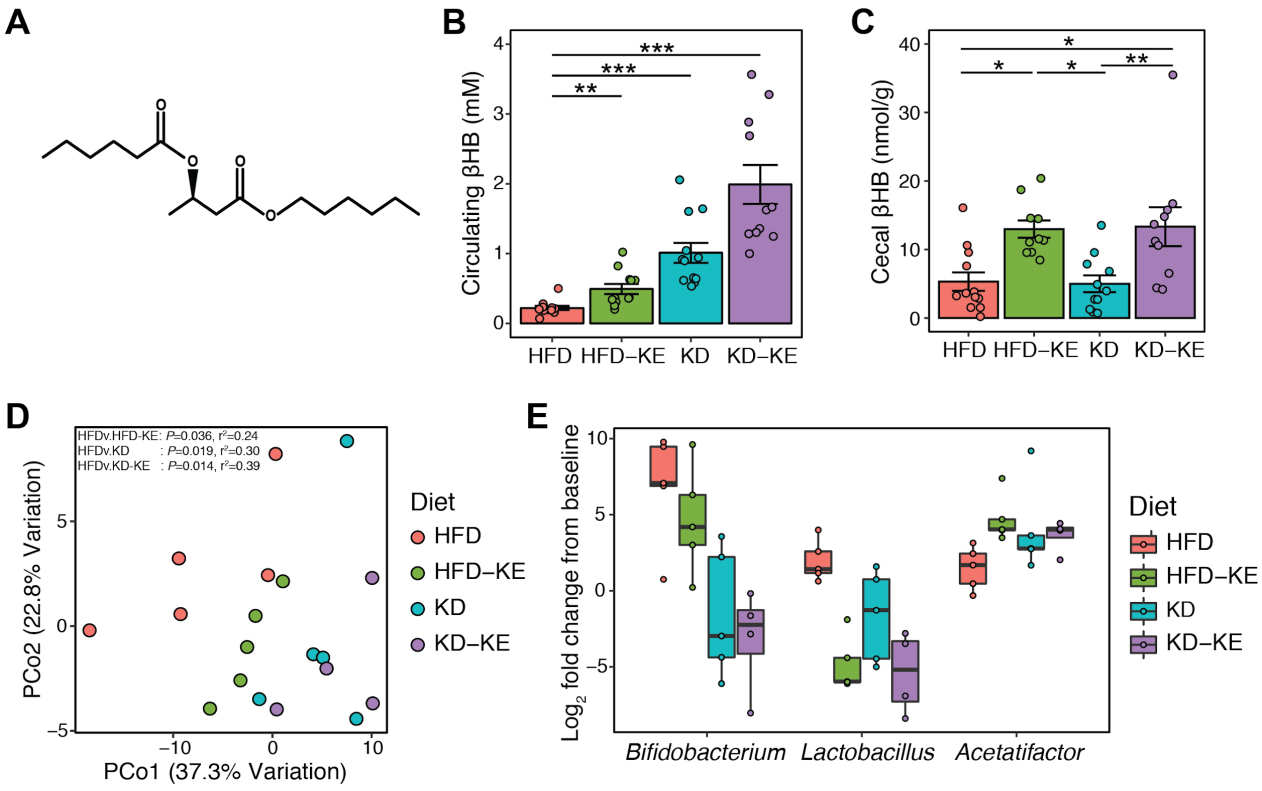

Figure 4.4. Ketone bodies alter gut microbial composition.
(A) Chemical structure of the ketone ester (KE) comprising β-hydroxybutyrate (βHB) linked to two 6-carbon medium chain fatty acids which are metabolized to βHB. (B) Circulating βHB levels in mice fed HFD, KE-supplemented HFD (HFD-KE), KD, or KE-supplemented KD (KD-KE) respectively for 3 weeks (n = 11-12 mice/group from two independent experiments, $^{**}P < 0.01$, $^{***}P < 0.001$; Welch's *t*-test comparing HFD to each of the other diets). (C) βHB concentration in cecal contents of mice fed HFD, KE-supplemented HFD (HFD-KE), KD, or KE-supplemented KD (KD-KE) respectively for 3 weeks (n = 11-12 mice/group from two independent experiments, $^{*}P < 0.05$, $^{**}P < 0.01$; one-way ANOVA with Tukey's test). (D) Principal coordinates analysis of PhILR Euclidean distances reveal distinct clustering of microbial communities between diet groups ($P = 0.001$, $r^2 = 0.41$, ADONIS), and microbial communities on the HFD diet are significantly different from each of the other diet groups (P and r^2 values are indicated on the PCoA plot, ADONIS). (E) Fold change of genera that are consistently altered in comparisons between HFD vs. KD and HFD vs. HFD-KE (FDR < 0.2, linear mixed effects model with MouseID as random effect), compared to baseline in the microbial communities of mice fed the respective diets (n = 4-5 mice/group).

Besides microbiota composition, I also monitored effects of the ketogenic diet and ketone ester (KE) supplementation on host physiology, namely food consumption and body composition. While the KE compound is well-suited for oral feeding, one caveat is that esters tend to have strong odors, and my preliminary studies suggest that it takes about one week for adult mice to adapt to the KE-supplemented diets, whereas mice adapt immediately to the ketogenic diet. Indeed, this was reflected in the first experiment I conducted using the KE-supplemented diets, where I observed that adult mice (aged 10 weeks at the start of the experiment) that were fed the KE-supplemented diets (HFD-KE and KD-KE) consumed significantly less calories compared to mice fed HFD or KD in the first week of feeding **(Figure 4.5A)**. The mice fully adapted to the diets after the first week, with no differences in calorie intake across the four diet groups observed in the second and final week of the experiment **(Figure 4.5A)**. In the second experiment where I started mice on diets at a younger age (5 weeks at the start of the experiment), there was no significant difference in calorie intake throughout the experimental course **(Figure 4.5C)**. This discrepancy in the first-week food consumption between the two experiments could suggest that the mice adapt more quickly to the odor of the KE at a younger age, though I have not specifically tested this hypothesis. More importantly, these observations suggest that the gut microbial differences observed with KE supplementation at experimental endpoint **(Figure 4.4D and 4.4E)** were not confounded by differences in caloric intake, a potential factor that influences microbiota composition (Jumpertz et al. 2011).

There was no significant difference in the body weights of mice fed HFD versus KD over three weeks; both diet groups gained weight steadily over the experimental

course **(Figure 4.5B and 4.5D)**. This observation that a normal-protein HFD and KD are obesogenic when fed continuously is consistent with prior reports (Newman et al. 2017; Borghjid and Feinman 2012). Although there were reports of mouse models of ketogenic diet that induced weight loss, these were later found to be attributed to extreme protein and/or vitamin deficiency in the diet design (Pissios et al. 2013; Schugar et al. 2013; Borghjid and Feinman 2012). It remains an open question as to why rodent models of ketogenic diets fail to recapitulate the weight loss effects observed in humans (Mansoor et al. 2016; Bueno et al. 2013); it is possible that ketogenic diets induce distinct metabolic responses between mice and humans. Given that the gut microbiome is a key regulator of host metabolism (Cani et al. 2019), differences in the bacterial species and strain-level metabolic capacities found in the gut microbiota of mice versus humans may also contribute to the divergent metabolic responses to KD.

Mice fed the KE-supplemented diets (HFD-KE and KD-KE) gained significantly less weight compared to mice fed HFD or KD **(Figure 4.5B and 4.5D)**. This could be accounted for by the lower food consumption in mice fed the KE-supplemented diets in the first week of diet **(Figure 4.5A)**, yet there was no overall differences in food consumption in the second experiment that could explain the lower body weight trajectory **(Figure 4.5C)** in mice fed HFD-KE compared to HFD. In fact, mice fed the HFD-KE diet gained significantly less adiposity compared to HFD-fed mice after three weeks **(Figure 4.5E)**, despite no significant differences in overall calorie intake throughout the dietary intervention **(Figure 4.5F)**. For future investigations, it would be interesting to study the effect of KE supplementation on energy expenditure, nutrient absorption or other factors that could mediate the observed differences in body weight and adiposity.

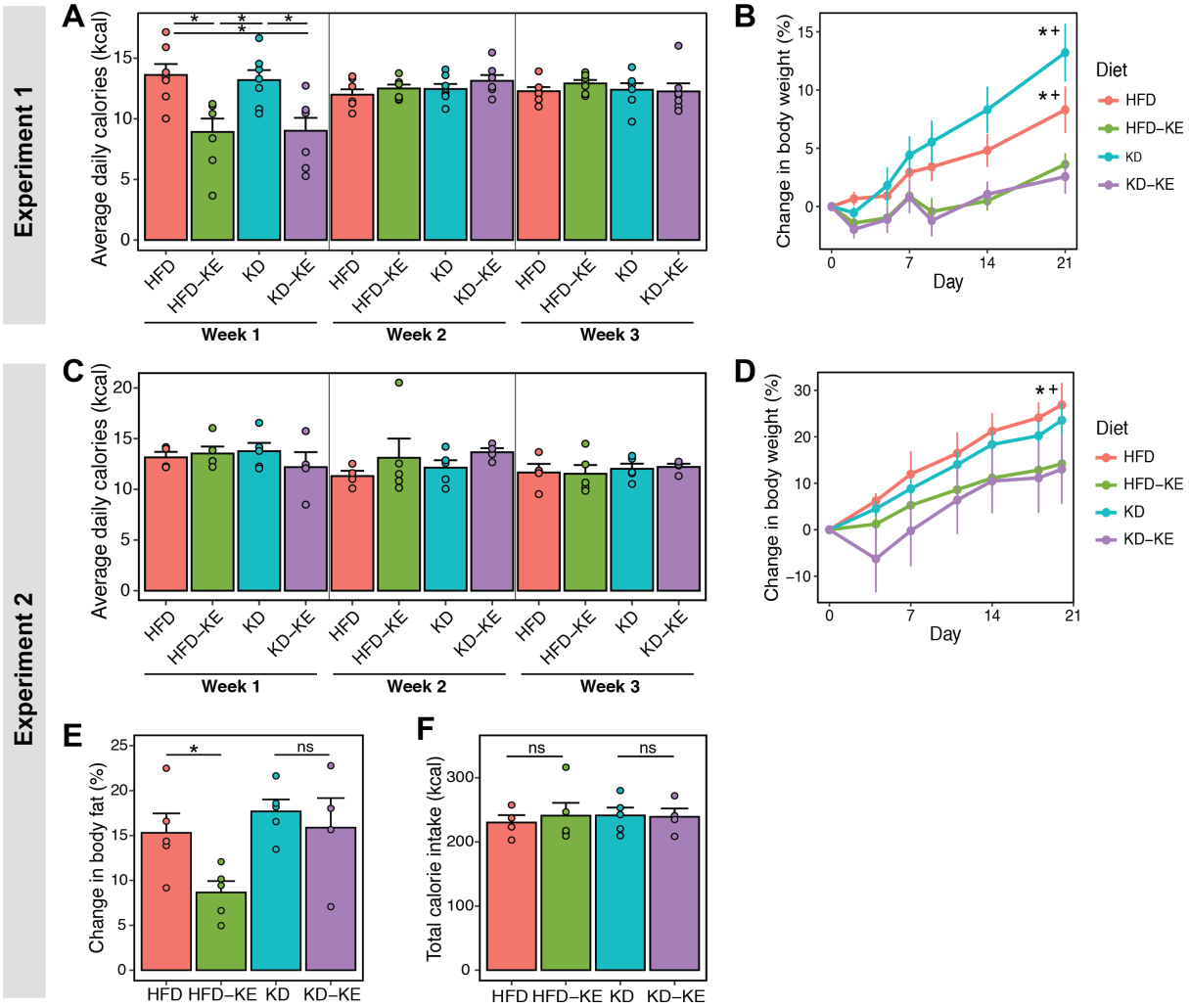

Figure 4.5. Effects of ketone ester feeding on host physiology.
(A) Daily calorie intake averaged per week in mice fed HFD, KE-supplemented HFD (HFD-KE), KD, or KE-supplemented KD (KD-KE) respectively for three weeks (n = 7 mice/group, *P < 0.05; one-way ANOVA with Tukey's test). (B) Body weight curves of mice fed the respective diets over three weeks (n = 7 mice/group, # and + symbols denote significant difference from HFD-KE and KD-KE respectively with significance determined as P < 0.05; two-way ANOVA comparing between diets over time). (C) Daily calorie intake was not significantly different between diet groups across all three weeks of dietary intervention (n = 4-5 mice/group; one-way ANOVA with Tukey's test). (D) Body weight curves of mice fed the respective diets over three weeks (n = 4-5 mice/group, # and + symbols denote significant difference from HFD-KE and KD-KE respectively with significance determined as P < 0.05; two-way ANOVA comparing between diets over time). (E) Change in adiposity determined using EchoMRI at the start and end of dietary intervention (n = 4-5 mice/group, *P < 0.05; unpaired t tests). (F) Total calorie intake over three weeks of dietary intervention (n = 4-5 mice/group, ns = not significant; unpaired t tests).

I next investigated whether βHB can directly impact bacterial growth *in vitro*, by comparing anaerobic growth with and without exogenous βHB across a panel of 35 gut bacterial isolates from 6 phyla **(Figure 4.6A)**, including bifidobacterial strains isolated from stool samples collected in our human study: two strains of *Bifidobacterium adolescentis* (strain BD1 and BD2) — the most abundant and prevalent species of *Bifidobacterium* in our human cohort **(Figure 2.2B)** — as well as *Bifidobacterium longum* (strain BD3) and *Bifidobacterium angulatum* (strain BD4). Each isolate was incubated with three different concentrations of βHB ranging from 12.5 - 50 μM and bacterial growth in rich media was quantified by optical density. For the majority of isolates, the concentration required to prevent ≥90% growth (MIC_{90}) occurred between 25 mM to 50 mM, with the exception of isolates in the genera *Eggerthella* and *Lactobacillus* that were insensitive to growth inhibition by βHB at the highest concentration tested (50 mM). On average, the *Bacteroidetes* tended to be sensitive to growth inhibition by βHB relative to the other phyla **(Figure 4.6B)**. It is worth noting that βHB concentrations used to achieve MIC_{90} in these bacterial monocultures exceed the physiological range — circulating βHB levels in humans rise up to 8 mM with prolonged starvation (Newman and Verdin 2017) — which suggests *in vitro* incubations of bacterial monocultures with βHB may not reflect the microenvironment or dynamics of complex communities found in the gut. Nevertheless, the ketogenic diet has been shown to increase levels of βHB in the intestinal tissue to the millimolar range (Tognini et al. 2017), which could suggest that bacteria residing close to the intestinal epithelium may be exposed to relatively high local concentrations of βHB similar to the concentrations tested in my *in vitro* assays.

Contrary to the selective reduction of *Bifidobacterium* and *Lactobacillus* observed *in vivo* with oral feeding of the ketone ester **(Figure 4.4E)**, I did not observe selective inhibition of either genera in the growth curve analyses. This suggests that the selective reduction of these genera observed *in vivo* could be a result of inter-species competition rather that direct inhibitory effects; for example, βHB may act as a signaling molecule (Newman and Verdin 2017) that alters the gene expression of microbial species in a way that causes *Bifidobacterium* and *Lactobacillus* to be outcompeted in the context of complex communities. Interestingly, I observed that βHB promoted the growth of a few bacterial isolates, for example the carrying capacity of *Eggerthella sinensis* and *Bifidobacterium animalis* were significantly increased in a dose-dependent manner by βHB **(Figure 4.6C**), which raises the intriguing possibility that some gut bacterial species could use βHB as a carbon source. In fact, although several genera of bacteria found in soil and other environments are known to synthesize and utilize a polymerized form of βHB known as poly-β-hydroxybutyrate (Braunegg, Lefebvre, and Genser 1998; S. Y. Lee 1996), this trait has not yet been characterized in gut bacteria. For future investigations, it would be interesting to further explore the mechanism-of-action of βHB on the physiology of gut bacteria, and to identify the genes that mediate either the inhibition or promotion of bacterial growth by βHB among gut bacterial strains.

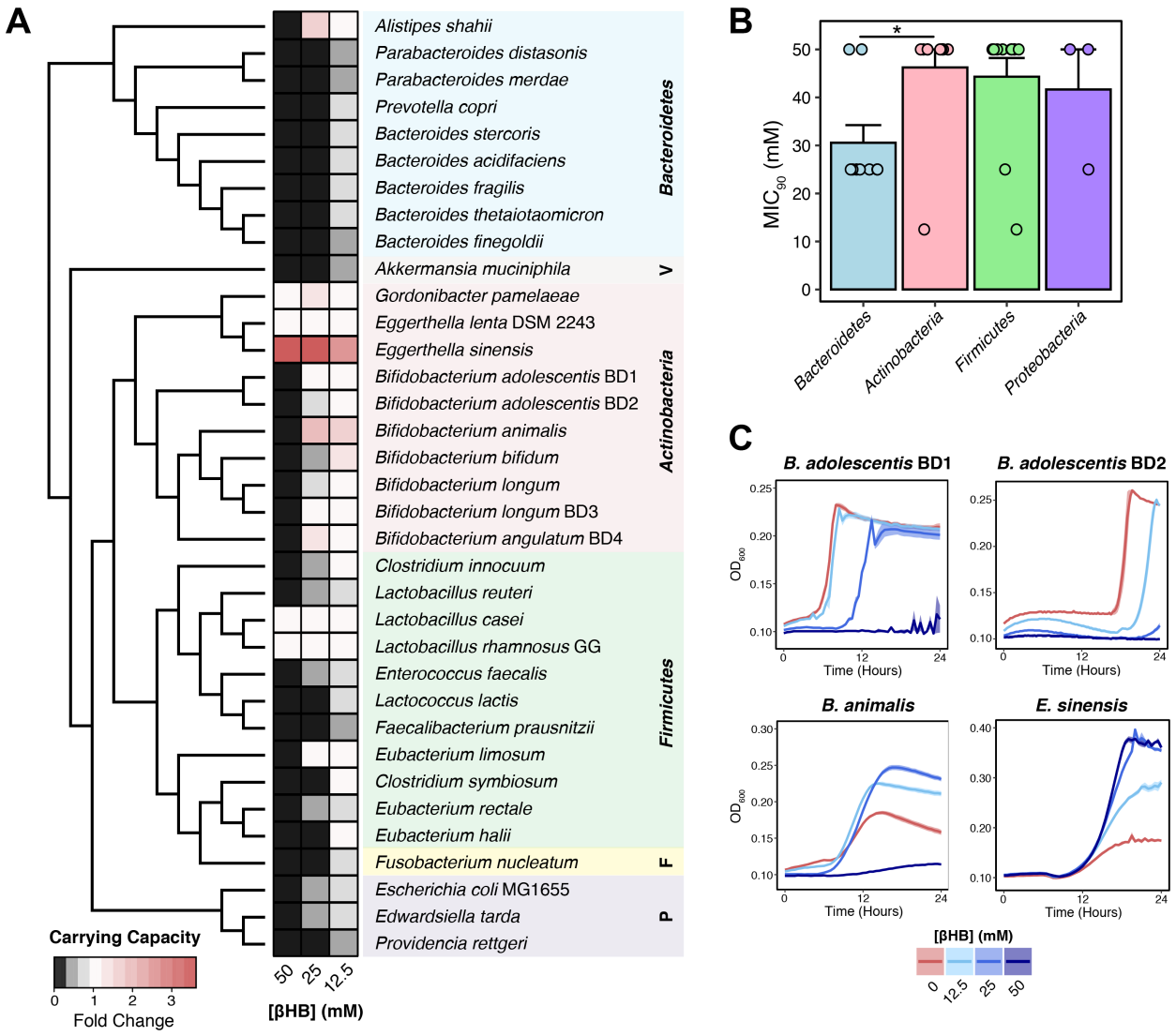

Figure 4.6. Strain variability in growth responses to βHB *in vitro*.

(A) A diverse panel of 35 gut bacterial isolates were incubated with varying concentrations of βHB, and a maximum likelihood phylogenetic tree using 16S rRNA gene sequences was constructed. Heatmap shows fold change of carrying capacity relative to media control at the respective βHB concentrations. F, *Fusobacteria*; V, *Verrucomicrobia*. (B) The minimum inhibitory concentration required to prevent ≥90% growth (MIC_{90}) of bacterial isolates spanning four major phyla. *Bacteroidetes* tended to be sensitive relative to the other phyla when tested in vitro (*P < 0.05; Kruskal-Wallis with Dunn's test). Mean±SEM shown. (C) Representative growth curves of selected isolates grown under anaerobic conditions with different concentrations of βHB. Growth curves show mean±SEM of triplicate cultures, with optical density (600 nM) measured at 15 min intervals over 24 hours.

Chapter 5.

Downstream consequences on host immunity

5.1 Mono-colonizations

A recent report showed that several *Bifidobacterium* species from the human gut microbiota, in particular *B. adolescentis*, are sufficient to robustly induce pro-inflammatory intestinal Th17 cells in mono-colonized mice (Tan et al. 2016). Given that I have showed a reproducible depletion of *Bifidobacterium* in both humans and mice fed KD as well as mice fed a ketone ester-supplemented HFD, I next asked if this could result in differences in intestinal Th17 cell accumulation in my studies. I mono-colonized germ-free mice with *B. adolescentis* BD1 (isolated from our human cohort) which resulted in a significant increase in Th17 cells in the small (but not large) intestines of mice **(Figure 5.1A)** that were fed a HFD over the course of the experiment, consistent with the published report (Tan et al. 2016). Consumption of a KD prevented the induction of intestinal Th17 cells in mice mono-colonized with *B. adolescentis* **(Figure 5.1B)**, consistent with a significant decrease in *B. adolescentis* colonization in the ileum compared to HFD-fed mice **(Figure 5.1C).** In contrast, Th1 cell levels were unaffected by KD consumption nor *B. adolescentis* mono-colonization **(Figure 5.1D)**; the latter is consistent with the previous report showing preferential induction of Th17 cells in the small intestine by *B. adolescentis (Tan et al. 2016)*. Taken together, these data suggest that host production of ketone bodies on a KD **(Figure 5.1E)** likely mediates the lack of intestinal Th17 induction in these mice by reducing colonization levels of *B. adolescentis*, and exemplifies the impact of diet-microbiota interactions on host immunity.

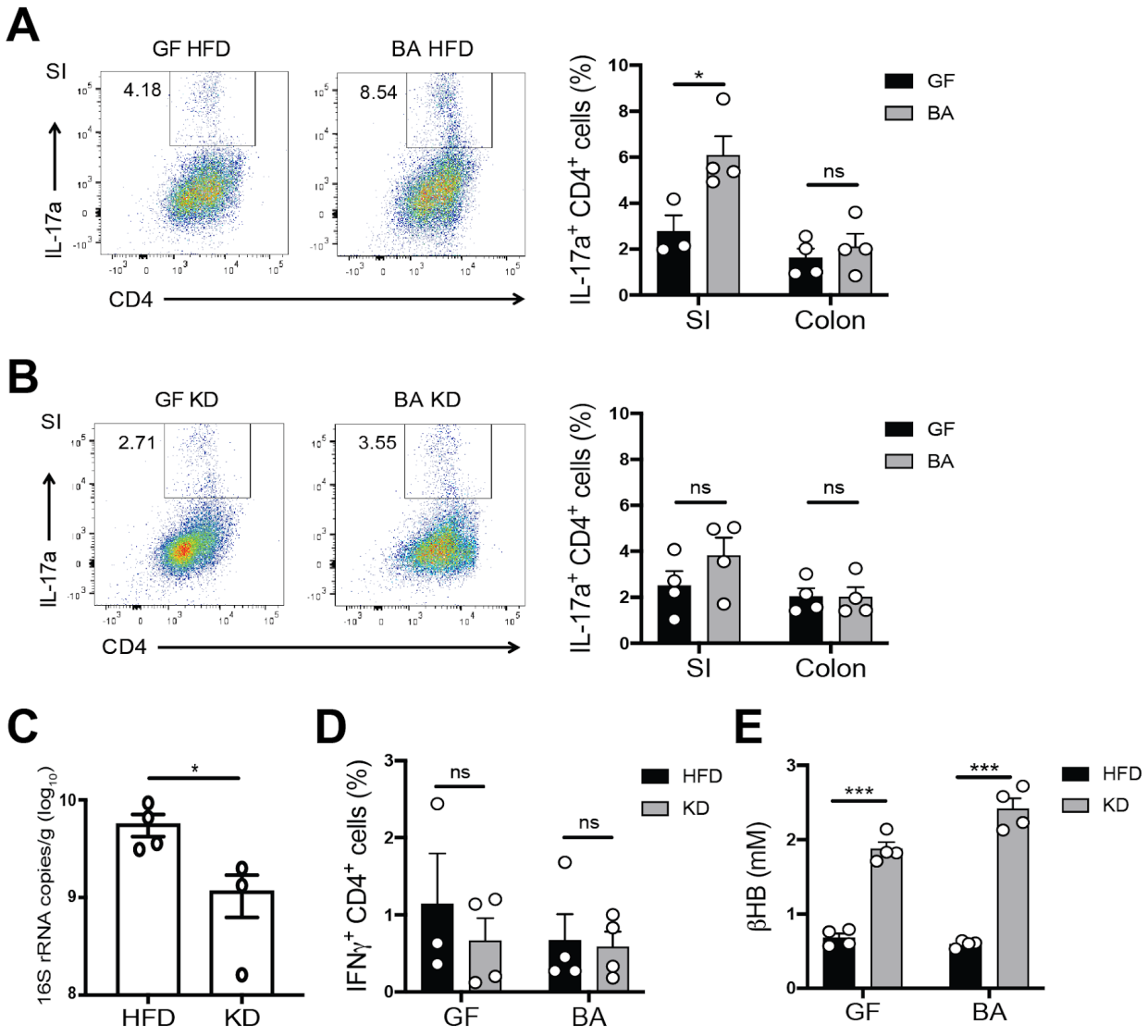

Figure 5.1. The ketogenic diet prevents intestinal Th17 induction by *Bifidobacterium adolescentis* in mono-colonized mice.
(A) *B. adolescentis* BD1 (BA) induces a robust Th17 population in the small intestine (SI) but not large intestine (colon) of mice fed HFD. Th17 populations are measured as IL-17a+ CD4+ live cell percentages. Black and grey bars represent germ-free (GF) and BA-monocolonized mice respectively (n = 4 mice/group, **P* < 0.05, ns = not significant; Welch's *t*-test). Representative flow cytometry plots of the IL-17a+ CD4+ live cell populations are shown to the left. (B) BA-monocolonized mice fed KD do not show intestinal Th17 cell induction compared to germ-free controls fed KD, in the small intestine and colon (n = 4 mice/group, ns = not significant; Welch's *t*-test). Representative flow cytometry plots of the IL-17a+ CD4+ live cell populations are shown to the left. (C) Bacterial DNA content, expressed as 16s rRNA gene copies/ gram wet weight in the ileal contents from BA-monocolonized mice fed HFD and KD respectively (n = 3-4 mice/group, **P* < 0.05; Welch's *t*-test). (D) Frequencies of Th1 cells in the small intestines are not significantly differently between GF and BA-monocolonized mice fed KD compared to

HFD. Black and grey bars represent HFD and KD respectively (n = 3-4 mice/group, ns = not significant; Welch's *t*-test). (E) Circulating βHB levels are significantly elevated in both GF and BA-monocolonized mice fed KD compared to HFD (n = 4 mice/group, ***P < 0.001; Welch's *t*-test). Data are presented as mean±SEM. Each data point represents an individual, singly-housed animal.

5.2 Human microbiota transplantations

I next wanted to investigate if changes in *Bifidobacterium* relative abundance in the context of an intact human gut microbiota would translate to differences in intestinal Th17 cell accumulation. I inoculated germ-free mice with fecal microbiota from human donors collected during the baseline diet (BD) or ketogenic diet (KD) stages respectively, and added a third experimental group in which I supplemented the KD-associated microbiota (itself containing a low relative abundance of *Bifidobacterium*) with *B. adolescentis* BD1 (KD+BA), thus recapitulating *Bifidobacterium* abundance in the BD microbiota at both phylum **(Figure 5.2A)** and genus level **(Figure 5.2B)** (CLR abundance of *Bifidobacterium* in donor community of BD: 8.14, KD: -2.56, KD+BA: 9.09). 16S rRNA gene sequencing of fecal samples showed that distinct microbial communities were established between BD and both KD microbiota groups (KD and KD+BA) which clustered similarly on the principal coordinates plot **(Figure 5.2C).** As expected, *Bifidobacterium* abundance was significantly lower in the KD group compared with either BD or KD+BA groups throughout the course of the experiment **(Figure 5.2D)**. Consistent with the observed differences in *Bifidobacterium* abundance, mice that received the KD microbiota showed significantly lower intestinal Th17 frequency **(Figure 5.2E)** compared to either BD or KD+BA groups**.** In contrast, there were no significant differences in the Th1 cell population **(Figure 5.2F)**. These results demonstrate that changes in the abundance of *Bifidobacterium* even in complex human gut microbial communities can have a meaningful impact on intestinal Th17 accumulation.

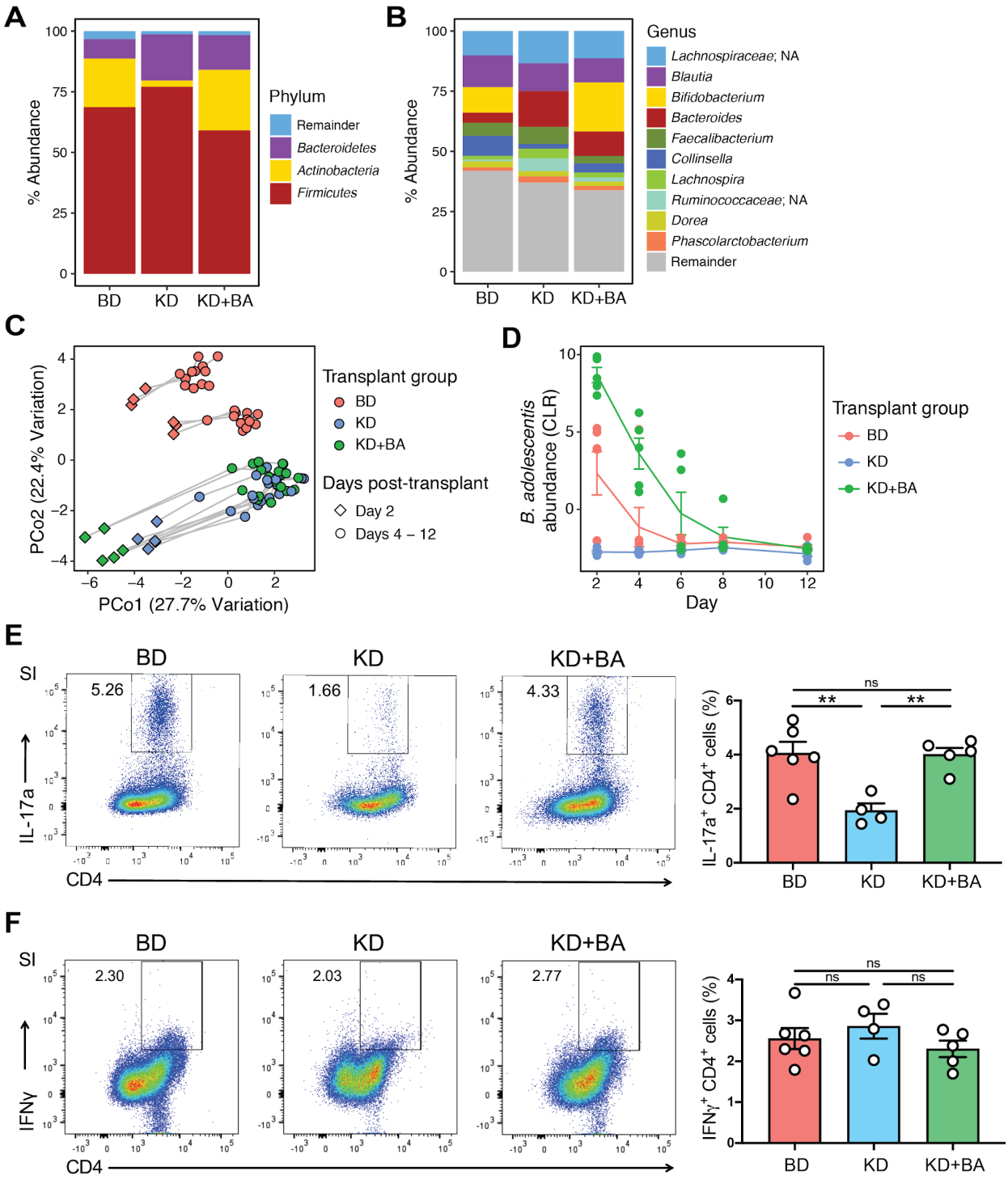

Figure 5.2. The KD-associated human microbiota reduces intestinal Th17 cell accumulation.

Community composition at (A) phylum and (B) genus level of donor fecal samples used for gnotobiotic transplant, pooled from the same four individuals during the baseline diet (BD) and ketogenic diet (KD) stages respectively, and a third sample comprising the KD donor sample supplemented with *B. adolescentis* BD1 (KD+BA). (C) Fecal microbiota of

mice colonized with the donor samples shown in panel A and B, sampled every two days post-transplant with sacrifice occurring 12 days post colonization (n = 5-6 mice/group). (D) Abundance of *B. adolescentis* (BA) in the fecal microbiota of mice in the three transplant groups, sampled over the course of the experiment (n = 5-6 mice/group). BA abundance is significantly different between transplant groups (P_{group} = 1.8e-5; $P_{KD+BAv.KD}$ < 0.001; $P_{KD+BAv.BD}$ < 0.01; $P_{BDv.KD}$ = 0.053). Statistical analysis carried out using linear mixed effects models (LMM) with MouseID as random effect and Tukey's test. (E) Mice that received the KD microbiota showed significantly lower levels of intestinal Th17 cells than either BD or KD+BA transplant groups. Representative flow cytometry plots of the IL-17a+ CD4+ live cell populations are shown to the left (n = 4-6 mice/group, $^{**}P < 0.01$, ns = not significant; one-way ANOVA with Tukey's test). (F) Th1 cell populations in the small intestine are not significantly different between transplant groups. Representative flow cytometry plots of the IFNγ+ CD4+ live cell populations are shown to the left (n = 4-6 mice/group, ns = not significant; one-way ANOVA with Tukey's test). Data are presented as mean±SEM. Each data point represents an individual, singly-housed animal.

5.3 Conventional mice

Given that human fecal transplantation of BD vs KD-associated microbiota was sufficient to reveal differential accumulation of Th17 cells in the gut, I hypothesized that differences in intestinal Th17 frequency should also be detectable in my diet experiments with conventional mice. Consistent with this hypothesis, conventional mice fed KD exhibited lower levels of Th17 cells in the small intestine (SI) compared to mice fed HFD **(Figures 5.3A and 5.3D)**. Similarly, mice fed the KE-supplemented HFD, which reduced *Bifidobacterium* abundance in the gut microbiota relative to HFD **(Figure 4.4E)**, led to lower Th17 cell accumulation in the small intestines **(Figure 5.3A)**. There were no differences in Th17 cell levels in the large intestines **(Figure 5.3B)** and spleen **(Figure 5.3C)**.

I also observed differences in SI Th17 cell accumulation with small changes in dietary carbohydrate intake **(Figure 3.4A)**, specifically, there was a significant drop in Th17 frequency in mice fed KD compared to those fed similar high-fat, low-carbohydrate diets **(Figure 5.3D)** that is consistent with a significant decrease in *Bifidobacterium* abundance **(Figure 5.3E)**. There was no significant changes in other immune cell subsets including Th1 **(Figure 5.3F)** and Treg **(Figure 5.3G)** cell populations, suggesting that the observed immune changes are specific to Th17 cells.

Given increasing evidence for immunological crosstalk between the gut and other tissue compartments (Y. S. Lee, Wollam, and Olefsky 2018; Winer et al. 2016; Powell, Walker, and Talley 2017; Morton et al. 2014), I wondered if the observed differences in Th17 responses in the gut could be detected more systemically. Although there was no difference in Th17 frequency in the spleen **(Figures 5.3C and 5.3H)**, there was a

significant drop in Th17 cell accumulation in visceral adipose tissue on both HFD89 (1% CHO) diet and KD compared to the other diets **(Figure 5.3l)**,. This provides initial evidence for a gut-adipose Th17 axis and is consistent with prior data suggesting that gut microbial-induced changes in the intestinal immune environment could in turn influence metabolic tissue inflammation (Winer et al. 2016; Y. S. Lee, Wollam, and Olefsky 2018). However, additional studies are warranted to control for circulating βHB which may directly decrease Th17 cells in adipose tissue (Puchalska and Crawford 2017). Regardless, these observations highlight how very-low-carbohydrate diets (0-1% CHO) are distinctive from low-carbohydrate diets (5-15% CHO) in both gut microbial and immune responses.

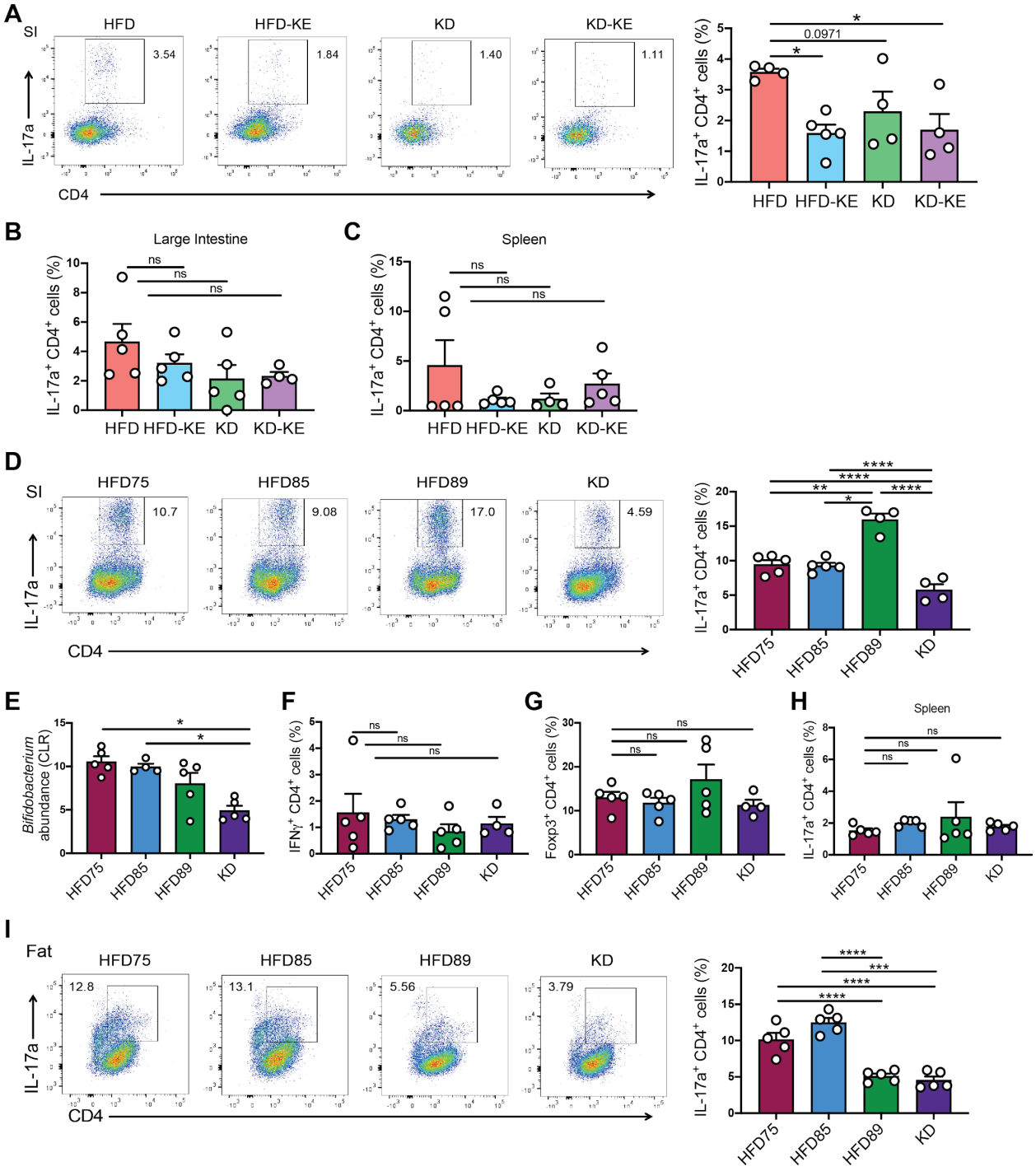

Figure 5.3. The ketogenic diet and ketone ester feeding reduces intestinal Th17 cell accumulation.

(A) Conventional mice fed either KD or ketone ester (KE)-supplemented diets show lower frequencies of small intestinal Th17 cells compared to mice fed HFD for 3 weeks (n = 4-5 mice/group, *P < 0.05; one-way ANOVA with Tukey's test). Representative flow cytometry plots of the IL-17a+ CD4+ live cell populations are shown to the left. Th17 cell levels were not significantly different in the (B) large intestine and (C) spleen (ns = not significant; one-way ANOVA with Tukey's test). (D) Conventional mice fed KD show

significantly lower Th17 cell accumulation compared to mice fed similar high-fat, low-carbohydrate diets shown in Figure 3.4A for 3 weeks (n = 4-5 mice/group, **P* < 0.05, ***P* < 0.01, *****P* < 0.0001; one-way ANOVA with Tukey's test). Representative flow cytometry plots of the IL-17a+ CD4+ live cell populations are shown to the left. (E) *Bifidobacterium* genus abundance in mice fed the respective diets (n = 4-5 mice/group, **P* < 0.05; Kruskal-Wallis with Dunn's test). (F) IFNγ+ CD4+ Th1 and (G) Foxp3+ CD4+ Treg cell populations in the small intestines were not significantly different between groups (ns = not significant; one-way ANOVA with Tukey's test). (H) No difference in Th17 cell accumulation in the spleen (ns = not significant; one-way ANOVA with Tukey's test). (I) Frequencies of Th17 cells in the epididymal white adipose tissue of mice fed the respective diets for 3 weeks (n = 4-5 mice/group, ****P* < 0.001, *****P* < 0.0001; one-way ANOVA with Tukey's test). Representative flow cytometry plots of the IL-17a+ CD4+ live cell populations in epididymal fat are shown to the left. Data are presented as mean±SEM. Each data point represents an individual, singly-housed animal.

Chapter 6.

Conclusions and future directions

In conclusion, my thesis work demonstrates how diet-induced changes in host-derived metabolites can alter the gut microbiota with downstream consequences for host immune responses. Through the combined use of controlled dietary interventions in humans and follow-on studies in conventional and gnotobiotic mice, I show that the impact of ketogenic diets on the gut microbiota are distinctive from that of high-fat diets. These changes appear to be driven not only by macronutrient intake but also by the concomitant host production of ketone bodies. Inhibition of bifidobacterial growth by ketone bodies results in KD-associated decreases in Th17 inflammation in the gut and adipose tissues in mice. Given the existing literature linking obesity with chronic low-grade inflammation in metabolic tissues (Hotamisligil 2017), decreased levels of pro-inflammatory Th17 cells in both gut and adipose tissues on a KD may be a potential mechanism contributing to the greater efficacy of KD in improving some aspects of metabolic syndrome such as glycemic control (Sainsbury et al. 2018; Saslow et al. 2017) and reductions in body fat (Mardinoglu et al. 2018; Volek et al. 2009). Furthermore, while previous work has demonstrated gut barrier disruption with consumption of HFHS diets which is associated with metabolic endotoxemia and inflammation (Everard et al. 2013), I found that KD maintained a robust mucus layer in mice despite the lack of fermentable carbohydrates, providing evidence that intestinal homeostasis is preserved on a KD.

The effects of long-term KD consumption on human health remain unclear, due to a lack of long-term studies tracking outcomes in humans adhering to a KD regimen. In mice, recent studies have shown long-term KD feeding to enhance longevity and reduce

disease onset in adult mice (Roberts et al. 2017; Newman et al. 2017). Aside from reported metabolic effects in short-term clinical trials in humans, KDs have been used as dietary treatment for intractable epilepsy since the 1920s and recent studies have found significantly positive outcomes with the use of KDs for treatment of refractory epilepsy in children and adults (Liu et al. 2018; Neal et al. 2008; Kverneland et al. 2015) where anti-epileptic drugs have failed. However, the mechanisms mediating the efficacy of KD as a treatment for epilepsy remain unknown. A recent paper provided intriguing evidence for the role of the gut microbiota in mediating anti-seizure effects of KD in mouse models of refractory epilepsy (Olson et al. 2018). Interestingly, another recent paper showed increased proportion of circulating Th17 cells in patients with intractable epilepsy compared to control individuals that was partially reversed following KD consumption (Ni et al. 2016), highlighting the potential role of Th17 immune responses in the pathogenesis of epilepsy, and consistent with my data showing decreased Th17 cell frequency in both the gut and adipose tissues with KD consumption. These observations together provide the premise for future investigations into the potential role of Th17 immune responses as a mechanism underlying the efficacy of KDs as treatment for refractory epilepsy and potentially other diseases associated with increased Th17 activation such as autoimmune diseases. More research is required to better understand the long-term consequences of KDs in humans in both health and disease.

This study highlights the role of the gut microbiota in mediating changes in intestinal Th17 cell responses to KD consumption, specifically I focused on *Bifidobacterium* which decreases in abundance during KD consumption in both humans and mice and also with feeding of a synthetic ketone ester in mice. I show that these

changes in *Bifidobacterium* abundances in the context of complex communities result in a significant alteration to intestinal Th17 cell populations, highlighting the role of *Bifidobacterium* in modulating adaptive immune responses. Importantly, the impact of diet and the gut microbiota on Th17 cells may be beneficial or detrimental depending on the context, warranting comparative analyses of these complex interactions in the context of inflammatory diseases (Tan et al. 2016), defense against enteric pathogens (Honda and Littman 2016), and cancer immunotherapy (Matson et al. 2018), among others. Further investigation is also needed to explore the potential consequences of changes in other members of the gut microbiota observed with KD consumption in our human cohort. Of note, both *Fusobacteria* and *Escherichia* were significantly enriched on the KD, which have both been implicated in predisposition to colorectal cancer (Kostic et al. 2013; Dalmasso et al. 2014). These results suggest that the short- and long-term impact of KDs on host health and disease likely depends upon a much more complex series of beneficial, neutral, and detrimental shifts in microbial ecology which remain to be explored.

It is worth noting that β-hydroxybutyrate (βHB) itself has anti-inflammatory effects due to its ability to inhibit the NLRP3 inflammasome (Puchalska and Crawford 2017). Thus, production of βHB during a KD could directly impact immune responses in addition to altering microbial mediated immunomodulation. Nevertheless, my thesis work provides evidence for a causal contribution of the gut microbiota in mediating the immune responses observed with KD consumption, as the transplantation of fecal microbiota from human donors fed KD versus a baseline diet into germ-free mice was sufficient to reveal differences in intestinal Th17 cell accumulation. My data supports the contribution of

select gut bacterial changes, specifically *Bifidobacterium*, in modulating the intestinal Th17 cell population, consistent with previous work which showed that *Bifidobacterium* robustly induced intestinal Th17 cells (Tan et al. 2016).

Although my investigations show that the gut microbial changes observed with KD consumption are mediated at least in part through host production of ketone bodies, future investigation is warranted to dissect the relative contribution of hepatic versus intestinal ketogenesis to the observed gut microbial changes. While local production of ketone bodies in the gut epithelium is likely to be more relevant to the gut microbiome and there is increased expression of ketogenic genes in the intestinal epithelium along with increased local concentrations of βHB with KD feeding (Tognini et al. 2017), it is possible that elevations of circulating βHB from hepatic production during KD could also directly or indirectly shape the gut microbiota. Elucidating the relative impact of intestinal versus hepatic ketogenesis on the gut microbiome might provide some insights into the physiological roles of ketone body production in the gut epithelium.

Overall, my thesis work extends important previous findings from our laboratory (David et al. 2014; Carmody et al. 2015) and others (Tan et al. 2016), providing evidence that the impact of diet on the gut microbiota is not only translatable from animal models to humans, but also appears to play a causal role in mediating host phenotypic responses to diet. Continued progress in elucidating the mechanistic basis for these observations could help inform more personalized approaches to utilize dietary interventions for the prevention and treatment of human disease.

Materials and methods

Diets

All diets were provided *ad libitum* unless otherwise noted. Semi-purified diets were purchased from Envigo. Diet codes and macronutrient compositions of the semi-purified diets used are listed in the table below. Standard chow diet (Lab Diet 5058) is used in the SPF facility, while standard autoclaved chow diet (Lab Diet 5021) is used in the gnotobiotic facility. All diets used for gnotobiotic experiments were either autoclaved or irradiated to ensure sterility.

Table S1. Macronutrient compositions of semi-purified diets used in this study

Diet	Diet Code	Macronutrient content (% kcal)		
		Protein	Carbohydrate	Fat
LFD	TD.150345	9.7	77.7	12.6
HFD75 (HFD)	TD.160239.PWD	9.8	15.0	75.2
HFD85	TD.180528.PWD	9.5	5.4	85.1
HFD89	TD.180527.PWD	9.5	1.4	89.1
KD	TD.160153.PWD	9.5	0.0	90.5
HFD-KE	TD.170411	10.0	15.2	71.3
KD-KE	TD.170412	9.6	0.0	87.4
LFD *RS	TD.160494	10.3	76.4	13.3
HFD45 *RS	TD.160495	10.2	43.3	46.6
HFD75 *RS	TD.160496	9.9	14.0	76.1

*RS = resistant starch

Bacteria Culturing Conditions

All bacteria were cultured at 37°C in an anaerobic chamber (Coy Laboratory Products) with an atmosphere composed of 2-3% H_2, 20% CO_2, and the balance N_2. Culture media was composed of brain heart infusion (BHI) media supplemented with *L*-cysteine-HCl

(0.05%, w/v), resazurin (0.0001%, w/v), hemin (5 µg/mL) and Vitamin K (1 µg/mL), referred to herein as BHI+ and allowed to equilibrate in the anaerobic environment prior to use.

Isolation of *Bifidobacteria*

Selective isolation of *Bifidobacteria* was carried out by plating diluted human fecal samples on TOS-propionate agar (Sigma) containing lithium-mupirocin supplement (Sigma), followed by incubation at 37°C overnight in an anaerobic Coy chamber. Single colonies were randomly selected and identified by Sanger sequencing of the full-length 16S rRNA gene. Identified bifidobacterial colonies were inoculated into fresh BHI media and incubated anaerobically for 24 hours, mixed with autoclaved glycerol and stored in a cryovial at -80°C until further use.

Bacterial Growth Curves

DL-β-Hydroxybutyric acid (Sigma 166898) was used for the *in vitro* bacterial growth studies. The βHB compound was dissolved in water and filter-sterilized to make 1M stock solutions. Two-fold serial dilutions of βHB were freshly prepared prior to the start of growth curve assays. 10 µL of each dilution or BHI+ media (for growth controls) were added in triplicate to wells of 96-well plates containing 40 µL of BHI+ media. Fresh cultures of bacteria were cultivated in BHI+ media at 37°C for 24 hours under anaerobic conditions, diluted to OD 0.01, then 50 µL of the diluted cultures were added to each well of 96-well plates except for sterile controls for which 50 µL of BHI+ media were added, making a total volume of 100 µL in each well. Plates were sealed with tape to minimize evaporation

and incubated at 37°C for 24 – 36 hours with continuous shaking, such that the growth controls for each isolate reached stationary phase. Growth curves were acquired by tracking OD at 600 nM with a microplate spectrophotometer (EON, BioTek Instruments), with measurements taken every 15 min. The minimal inhibitory concentration (MIC_{90}) was measured as the lowest concentration of βHB that resulted in >90% growth inhibition. Growth parameters including carrying capacity were calculated using the Growthcurver R package (Sprouffske and Wagner 2016).

Tree Construction

Ribosomal sequences for each isolate were extracted from the Ribosomal Database Project (RDP) (Cole et al. 2014) or generated from Sanger sequencing of the full-length 16S rRNA gene. Sequences were imported into UGENE (Okonechnikov et al. 2012) and aligned using MUSCLE (Edgar 2004). A maximum likelihood tree was generated using PhyML (Guindon et al. 2010) with 100 bootstraps and the GTR substitution model.

Gnotobiotic Colonization

B. adolescentis BD1 was inoculated into fresh BHI+ media and incubated at 37°C for 24 hours in an anaerobic Coy chamber. A single 200 µL aliquot of the *B. adolescentis* culture (1.3×10^8 cfu/mL) or sterile BHI+ media as vehicle control was administered by oral gavage into each germ-free mouse within its gnotobiotic isolator. Mice were switched from standard chow diet to either HFD or KD on the same day as colonization, and maintained on their respective diets during the 12-day experiment.

Fecal Microbiota Transplants

Four human donors were selected for fecal microbiota transplants, one from each study site. Frozen fecal samples from these human donors during BD and KD diet stages respectively were resuspended in 10 volumes (by weight) of BHI+ media in an anaerobic Coy chamber. Each diluted sample was vortexed for 1 min and left to settle for 5 min, and equal volumes of the clarified supernatants were pooled for gavage (one pool from four donor fecal samples collected during BD and a second pool containing another four samples collected from the same donors during KD). The KD microbiota pool was split into two volumes, and a third pool was prepared by spiking in fresh culture of *B. adolescentis* to one volume of the KD pool. A single 200 µL aliquot of each pooled sample was administered by oral gavage into each germ-free mouse within its gnotobiotic isolator. All mice were maintained on standard autoclaved chow diet over the 12-day experiment.

DNA Extraction

Human stool samples were homogenized with bead beating for 10 min on a vortex fitted with tube holder (MoBio, 13000-V1), using beads of mixed size and material (Lysing Matrix E 2mL Tube, MP Biomedicals) and the lysis solution provided in the PowerSoil bacterial DNA extraction kit (MoBio), and DNA was subsequently purified according to the manufacturer's instructions.

Mouse ileal and fecal samples were homogenized with bead beating for 5 min (Mini-Beadbeater-96, BioSpec) using the ZR BashingBead lysis matrix containing 0.1 and 0.5

mm beads (ZR-96 BashingBead Lysis Rack, Zymo Research) and the lysis solution provided in the ZymoBIOMICS 96 MagBead DNA Kit (Zymo Research). The samples were then centrifuged for 5 min at 3,000 g and the supernatant was transferred to 1mL deep-well plates. The DNA was then purified using the ZymoBIOMICS 96 MagBead DNA Kit (Zymo Research) according to manufacturer's instructions.

qPCR Assessment of Bacterial Loads

DNA was extracted as described above. Quantification against a standard curve of purified genomic DNA from *Escherichia coli* was performed by quantitative PCR of the V6 region using BioRad iTaq Universal Probes Supermix in triplicate 10 µL reactions using 200 nM of the following oligonucleotides: 5'-TGGAGCATGTGGTTTAATTCGA-3', 5'-TGCGGGACTTAACCCAACA-3', 5'-[Cy5]CACGAGCTGACGACARCCATGCA[BHQ3] -3'. Reactions were performed on a Bio-Rad CFX384 real-time thermocycler with the following cycle parameters: 95°C for 5 min followed by 40 cycles of 95°C for 5 sec, 60°C for 15 sec.

16S rRNA Sequencing and Analysis

DNA was isolated from human and mouse samples as described above. For human samples, 16S rRNA gene PCR was carried out using GoLay-barcoded 515F/806R primers (Caporaso et al. 2012) targeting the V4 region of the 16S rRNA gene according to the methods of the Earth Microbiome Project (earthmicrobiome.org). Amplicons were quantified with PicoGreen (Quant-It dsDNA, Life Technologies) and pooled at equimolar concentrations. For mouse samples, 16S rRNA gene PCR was carried out as per

reference protocol and primers (Gohl et al. 2016). Amplicons were pooled and normalized using the SequalPrep Normalization Plate Kit (Invitrogen). For both mouse and human samples, aliquots of the pools were then column (MinElute PCR Purification Kit, Qiagen) and gel purified (QIAquick Gel Extraction Kit, Qiagen). Libraries were then quantified and sequenced with a 600 cycle MiSeq Reagent Kit (250x250; Illumina) with ~15% PhiX.

Sequencing reads were demultiplexed using QIIME before denoising and processing with DADA2 (Callahan et al. 2016). Taxonomy was assigned using the DADA2 implementation of the RDP classifier (Wang et al. 2007) using the DADA2 formatted training sets for SILVA123 (benjjneb.github.io/dada2/assign.html). A phylogenetic tree was constructed using FastTree (Price, Dehal, and Arkin 2010) with midpoint rooting. Sequence variants were filtered such that they were present in more than one sample with at least a total of 10 reads. The PhILR Euclidean distance was calculated by first carrying out the phylogenetic isometric log ratio transformation (philr, PhILR (Silverman et al. 2017)) followed by calculating the Euclidean distance (vegdist, Vegan (Dixon 2003)). Principal coordinates analysis was carried out using the pcoa function of APE (Paradis, Claude, and Strimmer 2004). ADONIS calculations were carried out (adonis, Vegan) with 999 replications on each distance metric. The Wald test in DESeq2 package (Love, Huber, and Anders 2014) was used to analyze differential abundances on count data, using features that represented at least 0.05% of total sequencing reads. Centered log2-ratio (CLR) normalized abundances were calculated as $A_{clr}=[\log_2(A_1/g_a), \log_2(A_2/g_a),\ldots \log_2(A_n/g_a),]$, where A is a vector of read counts with a prior of 0.5 added and g_a is the geometric mean of all values of A. Time-course analysis of the ketone ester experiment

was carried out using linear mixed effects models (lmerTest, (Kuznetsova, Brockhoff, and Christensen 2017)) with mouse as a random effect to account for repeated sampling across time. Corrections for multiple hypothesis testing to false discovery rate (FDR) using the Benjamin-Hochberg method (Benjamini and Hochberg 1995) were performed where applicable.

Metagenomic Shotgun Sequencing and Analysis

Fecal DNA from human donors was isolated as described above. Whole-genome shotgun libraries were prepared using the Nextera XT DNA Library Prep Kit (Illumina). Paired ends of the libraries were sequenced on the Illumina HiSeq 2500 (Rapid Run mode) or NovaSeq 6000 platform. Raw Illumina reads underwent quality trimming and adaptor removal using Trimmomatic (Bolger, Lohse, and Usadel 2014) and host read removal by mapping to the human genome (GRCh38) with Bowtie2 (Langmead and Salzberg 2012). Taxonomic profiling and annotation was performed using MetaPhlAn2 (Segata et al. 2012).

Lamina Propria Lymphocyte Isolation

Lamina propria lymphocytes (LPLs) were isolated with slight modifications of previously described techniques (Atarashi et al. 2011; Round et al. 2011; Kubinak et al. 2015). In brief, small intestinal (SI) and colonic tissues were splayed longitudinally with mucus removed by scraping then stored in complete RPMI (10% fetal bovine serum, 100 units per mL penicillin and streptomycin, β-mercaptoethanol, glutamate, sodium pyruvate, HEPES and non-essential amino acids). Supernatants were discarded after filtering

through a 100 μM filter, and remaining tissue incubated in 1X HBSS (without $Ca^{2+}$and Mg^{2+}) containing 5 mM EDTA (Promega) and 1 mM DL-Dithiothreitol (DTT) (Bioplus chemicals) for 45 min at 37°C on a shaker. Supernatants were filtered through a 100μM filter and discarded, and remaining tissue was incubated for 45 min (colon) or 35 min (SI) at 37°C on a shaker in a solution containing 1X HBSS containing 5% (v/v) fetal bovine serum (GIBCO heat inactivated), 1 U/mL Dispase (Sigma), 0.5 mg/mL Collagenase VIII (Sigma), and 20 μg/mL DNaseI (Sigma). The supernatant was filtered over a 40 μm cell strainer into cold sterile 1X PBS. Cells were subjected to a Percoll (VWR) gradient (40%/80% [v/v] gradient) and spun at 2000 RPM for 20 min with no brake and no acceleration. Cells at the interface were collected, washed with PBS, and prepared for flow cytometry analysis.

Adipose Lymphocyte Isolation

Epididymal fat pads were dissected from the same side of mice following euthanasia and temporarily stored in 3 mL of cold Ham's F-10 medium prior to digestion. The tissues were then finely minced with scissors and digested in 3 mL of 2X digestion buffer (2 mg/mL at 250U/mg Collagenase type I, Worthington, and 30 mg/mL bovine serum albumin in Ham's F-10 medium) for 30 min at 37°C on a shaker, vortexing every 15 min. Cells were spun down at 1600 RPM for 7 min, resuspended in 10 mL of cold sterile 1X PBS, and filtered through a 40 μm cell strainer. Cells were spun down again, resuspended in PBS and prepared for flow cytometry analysis.

Flow Cytometry

LPLs were isolated from the colonic and SI lamina propria as described above. Fat lymphocytes were isolated as described above. For intracellular staining, cells were first stimulated with ionomycin (1000 ng/mL), PMA (50 ng/mL), and Golgi Plug (1 μL/sample) (BD Bioscience) overnight at 37°C. Stimulated cells were stained with LIVE/DEAD Fixable Aqua Dead Cell Stain Kit (Thermo Fisher) according to the manufacturer's instructions. Cells were surface stained with anti-CD3 (17A2, Invitrogen), anti-CD4 (GK1.5, Biolegend), washed, and then fixed/permeabilized in 100 μl Perm/Fix buffer (BD Bioscience). Cells were washed twice in Perm/Wash buffer (BD Bioscience) and then stained for intracellular cytokines: anti-Rorγt (B2D, Invitrogen), anti-IFNγ (XMG1.2, Millipore), anti-IL17a (ebio17B7, Invitrogen), anti-Foxp3 (150D, Biolegend). Cells were washed in Perm/Wash buffer twice and then re-suspended in staining buffer for flow cytometry analysis. Gating cell populations was done using isotype and single stain controls. These data were collected with a BD LSR Fortessa and analyzed with FlowJo software.

β-hydroxybutyrate (βHB) Measurements

Blood was obtained from mice by cardiac puncture immediately following euthanasia in the day between 9am till noon. Blood was collected into collection tubes coated with K_2-EDTA (Terumo T-MQK) or with serum separator (BD Microtainer 365978), centrifuged at 13,000 RPM for 10 min at 4°C to separate the plasma or serum, and frozen at −20°C until use. βHB levels were quantified using the StanBio LiquiColor Beta-Hydroxybutyrate colorimetric test (StanBio) according to the manufacturer's instructions. Baseline

absorbance of the sample-enzyme mixture prior to adding catalyst were subtracted from the final absorbance values in order to account for any sample hemolysis, with 2-3 replicates run per sample.

Ketone Ester Synthesis

The synthesis method for the hexanoyl hexyl β-hydroxybutyrate (C6x2-βHB) ester was developed by Scott Ulrich of Ithaca College (Ithaca, New York, USA), and the ester was then custom ordered in bulk from AK Scientific (Union City, CA). The βHB moiety of the ester is chiral, and the compound was synthesized as an enantiomeric mixture. Briefly, hexyl β-hydroxybutyrate was prepared by suspending sodium β-hydroxybutyrate in dry dimethylformamide and reacting with 1-bromohexane, followed by hexyl acyl chloride. The identity of the final product was confirmed by ^{1}H NMR and gas chromatograph mass spectrometry (GC/MS), with 97.5% purity on GC.

NMR Global Metabolomics

NMR spectroscopy was performed at 298K on a Bruker Avance III 600-MHz spectrometer configured with a 5 mm inverse cryogenic probe (Bruker Biospin, Germany) as previously described (Cai et al. 2017). 50 mg of fresh human feces were extracted with 1 mL of phosphate buffer (K_2HPO_4/NaH_2PO_4, 0.1 M, pH 7.4, 50% v/v D2O) containing 0.005% sodium 3-(trimethylsilyl) [2,2,3,3-2H4] propionate (TSP-d_4) as a chemical shift reference (δ 0.00). Samples were freeze-thawed three times with liquid nitrogen and water bath for thorough extraction, then homogenized (6500 rpm, 1 cycle, 60s) and centrifuged (11 180g, 4 °C, 10 min). The supernatants were transferred to a new 2 mL tube. Additional

600 µL of PBS was added to the pellets, followed by the same extraction procedure described above. Combined fecal extracts were centrifuged (11,180g, 4 °C, 10 min), 600 µL supernatants were transferred to a 5 mm NMR tube (Norell, Morganton, NC) for NMR spectroscopy analysis. A standard one-dimensional NOESY pulse sequence noesypr1d (recycle delay-90°-t1-90°-tm-90°-acquisition) is used with a 90 pulse length of approximately 10s (-9.6 dbW) and 64 transients are recorded into 32k data points with a spectral width of 9.6 KHz.

NMR Spectra are processed as previously described (Cai et al. 2017). First, all spectra quality was improved with topspin 3.0 (Bruker Biospin, Germany) for phase and baseline correction and chemical shift calibration. Then AMIX software (version: 3.9.14, Brucker Biospin, Germany) was used for bucketing (bucket width 0.004 ppm), interference signal removing (water and polyethylene glycol), and scaling (total intensity). The following multivariate data analysis was performed with SIMCA 13 (Umetrics, Sweden). Orthogonal projection to latent structure-discriminant analysis (OPLS-DA) was performed with UV scaling, and the model was validated with a 7-fold cross validation method. R^2X and Q^2 values generated from the method represent the predictive power and validity of the models, respectively.

Targeted Bile Acid Quantitation by UPLC-MS/MS

Bile acids quantitation in mouse cecal content, serum and human feces was performed with an ACQUITY UPLC using a BEH C8 column (1,7 µm, 100 mm x 2.1 mm) coupled with a Xevo TQ-S mass spectrometer equipped with an electrospray ionization (ESI)

source operating in negative mode (All Waters, Milford, MA) as previously described (Sarafian et al. 2015). Selected ion monitoring (SIR) for non-conjugated bile acid and multiple reaction monitoring (MRM) for conjugated bile acid were used. 50 mg of cecal content/feces was pre-weighed, mixed with 1 mL of pre-cooled methanol containing 0.5 μM stable-isotope-labeled bile acids (internal standards) and 1.0 mm diameter zirconia/silica beads (BioSpec, Bartlesville, OK), followed by thorough homogenization and centrifugation. Supernatant was transferred to an autosampler vial for analysis. 100 μL of serum was extracted by adding 200 μL pre-cooled methanol containing 0.5 μM internal standard bile acids. Following centrifugation, the supernatant of the extract was transferred to an autosampler vial for quantitation. Calibration curves of individual bile acids were drafted with bile acid standards for quantitation of the biological abundance of bile acids.

RNA Extraction and qPCR Analysis for Gene Expression

Total RNA was isolated from colonic tissues using the Direct-zol-96 MagBead kit (Zymo Research) as per the manufacturer's instructions. For qPCR analysis, cDNA was synthesized using iScript Reverse Transcription Supermix (Bio-Rad), and qPCR was performed using a commercially available TaqMan Gene Expression Assay for *Muc2* (Assay ID: Mm01276694_g1) with iTaq Universal Probes Supermix (Bio-Rad) on a Bio-Rad CFX384 real-time thermocycler. Samples were run in triplicates and normalized to the *B2m* housekeeping gene (Taqman Gene Expression Assay ID: Mm00437762_m1).

Intestinal Tissue Collection, Fixation and Processing

Sections of the distal colon, closest to the rectum and containing a fecal pellet, were collected from mice following euthanasia and placed in cassettes. Tissues were fixed in methacarn solution and processed as previously described (Johansson and Hansson 2012; Earle et al. 2015). Colon samples within cassettes were then submerged in melted paraffin at 68°C for 1 hr, removed, and kept at room temperature until sectioning. Paraffin blocks were cut into 4-µm-thick sections and deparaffinized for FISH staining.

Fluorescence *In Situ* Hybridization (FISH) Preparation

FISH was performed as previously described (Johansson and Hansson 2012; Earle et al. 2015). Briefly, deparaffinized sections were incubated with the universal bacterial EUB338 probe (Amann et al. 1990) diluted to 10ng/µl in hybridization buffer (0.9 M NaCl, 20 mM Tris-HCl [pH 7.4], 0.01% sodium dodecyl sulfate, 10% formamide) at 50°C for 20 min in the dark and washed three times in PBS. Samples were then incubated with 10µg/mL DAPI (EMD Millipore) and 40µg/mL FITC-UEA1 (Sigma) in the dark for 1 hr at 4°C, washed three times in PBS, allowed to dry, and mounted in Vectashield mounting medium (Vector Labs).

Imaging and Quantitation of Mucus Layer in Colon Sections

Images were acquired on a Zeiss LSM 880 or Leica SP5 confocal microscope. Samples were imaged with a 63x oil-immersion objective. For quantification of mucus thickness, images were acquired with a frame size of 1912 X 1912 and 16-bit depth on the Zeiss LSM 880 microscope, with tile scans acquired using a mechanical stage and overlapping

images (3 x 5) stitched using the ZEN Imaging Software (black edition). Mucus thickness was then quantified using the analysis platform BacSpace (Earle et al. 2015).

Datasets Generated and Deposited

All sequencing datasets generated in the current study are deposited in the NCBI Sequence Read Archive under BioProject PRJNA529487.

References

Amann, R. I., B. J. Binder, R. J. Olson, S. W. Chisholm, R. Devereux, and D. A. Stahl. 1990. "Combination of 16S rRNA-Targeted Oligonucleotide Probes with Flow Cytometry for Analyzing Mixed Microbial Populations." *Applied and Environmental Microbiology* 56 (6): 1919–25.

Atarashi, Koji, Takeshi Tanoue, Tatsuichiro Shima, Akemi Imaoka, Tomomi Kuwahara, Yoshika Momose, Genhong Cheng, et al. 2011. "Induction of Colonic Regulatory T Cells by Indigenous Clostridium Species." *Science* 331 (6015): 337–41.

Bäckhed, Fredrik, Hao Ding, Ting Wang, Lora V. Hooper, Gou Young Koh, Andras Nagy, Clay F. Semenkovich, and Jeffrey I. Gordon. 2004. "The Gut Microbiota as an Environmental Factor That Regulates Fat Storage." *Proceedings of the National Academy of Sciences of the United States of America* 101 (44): 15718–23.

Benjamini, Yoav, and Yosef Hochberg. 1995. "Controlling the False Discovery Rate: A Practical and Powerful Approach to Multiple Testing." *Journal of the Royal Statistical Society. Series B, Statistical Methodology* 57 (1): 289–300.

Bisanz, Jordan E., Vaibhav Upadhyay, Jessie A. Turnbaugh, Kimberly Ly, and Peter J. Turnbaugh. 2019. "Diet Induces Reproducible Alterations in the Mouse and Human Gut Microbiome." *bioRxiv*. https://doi.org/10.1101/541797.

Bolger, Anthony M., Marc Lohse, and Bjoern Usadel. 2014. "Trimmomatic: A Flexible Trimmer for Illumina Sequence Data." *Bioinformatics* 30 (15): 2114–20.

Borghjid, Saihan, and Richard David Feinman. 2012. “Response of C57Bl/6 Mice to a Carbohydrate-Free Diet.” *Nutrition & Metabolism* 9 (1): 69.

Braunegg, G., G. Lefebvre, and K. F. Genser. 1998. “Polyhydroxyalkanoates, Biopolyesters from Renewable Resources: Physiological and Engineering Aspects.” *Journal of Biotechnology* 65 (2-3): 127–61.

Bueno, Nassib Bezerra, Ingrid Sofia Vieira de Melo, Suzana Lima de Oliveira, and Terezinha da Rocha Ataide. 2013. “Very-Low-Carbohydrate Ketogenic Diet v. Low-Fat Diet for Long-Term Weight Loss: A Meta-Analysis of Randomised Controlled Trials.” *The British Journal of Nutrition* 110 (7): 1178–87.

Cai, Jingwei, Jingtao Zhang, Yuan Tian, Limin Zhang, Emmanuel Hatzakis, Kristopher W. Krausz, Philip B. Smith, Frank J. Gonzalez, and Andrew D. Patterson. 2017. “Orthogonal Comparison of GC-MS and 1H NMR Spectroscopy for Short Chain Fatty Acid Quantitation.” *Analytical Chemistry* 89 (15): 7900–7906.

Callahan, Benjamin J., Paul J. McMurdie, Michael J. Rosen, Andrew W. Han, Amy Jo A. Johnson, and Susan P. Holmes. 2016. “DADA2: High-Resolution Sample Inference from Illumina Amplicon Data.” *Nature Methods* 13 (7): 581–83.

Cani, Patrice D., Jacques Amar, Miguel Angel Iglesias, Marjorie Poggi, Claude Knauf, Delphine Bastelica, Audrey M. Neyrinck, et al. 2007. “Metabolic Endotoxemia Initiates Obesity and Insulin Resistance.” *Diabetes* 56 (7): 1761–72.

Cani, Patrice D., Matthias Van Hul, Charlotte Lefort, Clara Depommier, Marialetizia Rastelli, and Amandine Everard. 2019. “Microbial Regulation of Organismal Energy Homeostasis.”

Nature Metabolism 1 (1): 34–46.

Caporaso, J. Gregory, Christian L. Lauber, William A. Walters, Donna Berg-Lyons, James Huntley, Noah Fierer, Sarah M. Owens, et al. 2012. “Ultra-High-Throughput Microbial Community Analysis on the Illumina HiSeq and MiSeq Platforms.” *The ISME Journal* 6 (8): 1621–24.

Carmody, Rachel N., Georg K. Gerber, Jesus M. Luevano Jr, Daniel M. Gatti, Lisa Somes, Karen L. Svenson, and Peter J. Turnbaugh. 2015. “Diet Dominates Host Genotype in Shaping the Murine Gut Microbiota.” *Cell Host & Microbe* 17 (1): 72–84.

Clarke, Kieran, Kirill Tchabanenko, Robert Pawlosky, Emma Carter, M. Todd King, Kathy Musa-Veloso, Manki Ho, et al. 2012. “Kinetics, Safety and Tolerability of (R)-3-Hydroxybutyl (R)-3-Hydroxybutyrate in Healthy Adult Subjects.” *Regulatory Toxicology and Pharmacology: RTP* 63 (3): 401–8.

Cole, James R., Qiong Wang, Jordan A. Fish, Benli Chai, Donna M. McGarrell, Yanni Sun, C. Titus Brown, Andrea Porras-Alfaro, Cheryl R. Kuske, and James M. Tiedje. 2014. “Ribosomal Database Project: Data and Tools for High Throughput rRNA Analysis.” *Nucleic Acids Research* 42 (Database issue): D633–42.

Dalmasso, Guillaume, Antony Cougnoux, Julien Delmas, Arlette Darfeuille-Michaud, and Richard Bonnet. 2014. “The Bacterial Genotoxin Colibactin Promotes Colon Tumor Growth by Modifying the Tumor Microenvironment.” *Gut Microbes* 5 (5): 675–80.

David, Lawrence A., Corinne F. Maurice, Rachel N. Carmody, David B. Gootenberg, Julie E. Button, Benjamin E. Wolfe, Alisha V. Ling, et al. 2014. “Diet Rapidly and Reproducibly

Alters the Human Gut Microbiome." *Nature* 505 (7484): 559–63.

Desai, Mahesh S., Anna M. Seekatz, Nicole M. Koropatkin, Nobuhiko Kamada, Christina A. Hickey, Mathis Wolter, Nicholas A. Pudlo, et al. 2016. "A Dietary Fiber-Deprived Gut Microbiota Degrades the Colonic Mucus Barrier and Enhances Pathogen Susceptibility." *Cell* 167 (5): 1339–53.e21.

Dixon, Philip. 2003. "VEGAN, a Package of R Functions for Community Ecology." *Journal of Vegetation Science: Official Organ of the International Association for Vegetation Science* 14 (6): 927–30.

Earle, Kristen A., Gabriel Billings, Michael Sigal, Joshua S. Lichtman, Gunnar C. Hansson, Joshua E. Elias, Manuel R. Amieva, Kerwyn Casey Huang, and Justin L. Sonnenburg. 2015. "Quantitative Imaging of Gut Microbiota Spatial Organization." *Cell Host & Microbe* 18 (4): 478–88.

Edgar, Robert C. 2004. "MUSCLE: Multiple Sequence Alignment with High Accuracy and High Throughput." *Nucleic Acids Research* 32 (5): 1792–97.

Everard, Amandine, Clara Belzer, Lucie Geurts, Janneke P. Ouwerkerk, Céline Druart, Laure B. Bindels, Yves Guiot, et al. 2013. "Cross-Talk between Akkermansia Muciniphila and Intestinal Epithelium Controls Diet-Induced Obesity." *Proceedings of the National Academy of Sciences of the United States of America* 110 (22): 9066–71.

Frank, Daniel N., Allison L. St Amand, Robert A. Feldman, Edgar C. Boedeker, Noam Harpaz, and Norman R. Pace. 2007. "Molecular-Phylogenetic Characterization of Microbial Community Imbalances in Human Inflammatory Bowel Diseases." *Proceedings*

of the National Academy of Sciences of the United States of America 104 (34): 13780–85.

Gohl, Daryl M., Pajau Vangay, John Garbe, Allison MacLean, Adam Hauge, Aaron Becker, Trevor J. Gould, et al. 2016. “Systematic Improvement of Amplicon Marker Gene Methods for Increased Accuracy in Microbiome Studies.” *Nature Biotechnology* 34 (9): 942–49.

Guindon, Stéphane, Jean-François Dufayard, Vincent Lefort, Maria Anisimova, Wim Hordijk, and Olivier Gascuel. 2010. “New Algorithms and Methods to Estimate Maximum-Likelihood Phylogenies: Assessing the Performance of PhyML 3.0.” *Systematic Biology* 59 (3): 307–21.

Hall, Kevin D., Kong Y. Chen, Juen Guo, Yan Y. Lam, Rudolph L. Leibel, Laurel Es Mayer, Marc L. Reitman, et al. 2016. “Energy Expenditure and Body Composition Changes after an Isocaloric Ketogenic Diet in Overweight and Obese Men.” *The American Journal of Clinical Nutrition* 104 (2): 324–33.

Hall, Kevin D., and Stephanie T. Chung. 2018. “Low-Carbohydrate Diets for the Treatment of Obesity and Type 2 Diabetes.” *Current Opinion in Clinical Nutrition and Metabolic Care* 21 (4): 308–12.

Honda, Kenya, and Dan R. Littman. 2016. “The Microbiota in Adaptive Immune Homeostasis and Disease.” *Nature* 535 (7610): 75–84.

Hotamisligil, Gökhan S. 2017. “Inflammation, Metaflammation and Immunometabolic Disorders.” *Nature* 542 (7640): 177–85.

Johansson, Malin E. V., and Gunnar C. Hansson. 2012. “Preservation of Mucus in

Histological Sections, Immunostaining of Mucins in Fixed Tissue, and Localization of Bacteria with FISH." In *Mucins: Methods and Protocols*, edited by Michael A. McGuckin and David J. Thornton, 229–35. Totowa, NJ: Humana Press.

Jumpertz, Reiner, Duc Son Le, Peter J. Turnbaugh, Cathy Trinidad, Clifton Bogardus, Jeffrey I. Gordon, and Jonathan Krakoff. 2011. "Energy-Balance Studies Reveal Associations between Gut Microbes, Caloric Load, and Nutrient Absorption in Humans." *The American Journal of Clinical Nutrition* 94 (1): 58–65.

Koeth, Robert A., Zeneng Wang, Bruce S. Levison, Jennifer A. Buffa, Elin Org, Brendan T. Sheehy, Earl B. Britt, et al. 2013. "Intestinal Microbiota Metabolism of L-Carnitine, a Nutrient in Red Meat, Promotes Atherosclerosis." *Nature Medicine* 19 (5): 576–85.

Kostic, Aleksandar D., Eunyoung Chun, Lauren Robertson, Jonathan N. Glickman, Carey Ann Gallini, Monia Michaud, Thomas E. Clancy, et al. 2013. "Fusobacterium Nucleatum Potentiates Intestinal Tumorigenesis and Modulates the Tumor-Immune Microenvironment." *Cell Host & Microbe* 14 (2): 207–15.

Kubinak, Jason L., Charisse Petersen, W. Zac Stephens, Ray Soto, Erin Bake, Ryan M. O'Connell, and June L. Round. 2015. "MyD88 Signaling in T Cells Directs IgA-Mediated Control of the Microbiota to Promote Health." *Cell Host & Microbe* 17 (2): 153–63.

Kuznetsova, Alexandra, Per Brockhoff, and Rune Christensen. 2017. "lmerTest Package: Tests in Linear Mixed Effects Models." *Journal of Statistical Software, Articles* 82 (13): 1–26.

Kverneland, Magnhild, Kaja K. Selmer, Karl O. Nakken, Per O. Iversen, and Erik Taubøll.

2015. “A Prospective Study of the Modified Atkins Diet for Adults with Idiopathic Generalized Epilepsy.” *Epilepsy & Behavior: E&B* 53 (December): 197–201.

Lam, Kathy N., Margaret Alexander, and Peter J. Turnbaugh. 2019. “Precision Medicine Goes Microscopic: Engineering the Microbiome to Improve Drug Outcomes.” *Cell Host & Microbe* 26 (1): 22–34.

Langmead, Ben, and Steven L. Salzberg. 2012. “Fast Gapped-Read Alignment with Bowtie 2.” *Nature Methods* 9 (4): 357–59.

Lee, S. Y. 1996. “Bacterial Polyhydroxyalkanoates.” *Biotechnology and Bioengineering* 49 (1): 1–14.

Lee, Yun Sok, Joshua Wollam, and Jerrold M. Olefsky. 2018. “An Integrated View of Immunometabolism.” *Cell* 172 (1-2): 22–40.

Liu, Hongyan, Yi Yang, Yunbing Wang, Hong Tang, Fan Zhang, Yong Zhang, and Yong Zhao. 2018. “Ketogenic Diet for Treatment of Intractable Epilepsy in Adults: A Meta-Analysis of Observational Studies.” *Epilepsia Open* 3 (1): 9–17.

Love, Michael I., Wolfgang Huber, and Simon Anders. 2014. “Moderated Estimation of Fold Change and Dispersion for RNA-Seq Data with DESeq2.” *Genome Biology* 15 (12): 550.

Mansoor, Nadia, Kathrine J. Vinknes, Marit B. Veierød, and Kjetil Retterstøl. 2016. “Effects of Low-Carbohydrate Diets v. Low-Fat Diets on Body Weight and Cardiovascular Risk Factors: A Meta-Analysis of Randomised Controlled Trials.” *The British Journal of Nutrition* 115 (3): 466–79.

Mardinoglu, Adil, Hao Wu, Elias Bjornson, Cheng Zhang, Antti Hakkarainen, Sari M.

Räsänen, Sunjae Lee, et al. 2018. “An Integrated Understanding of the Rapid Metabolic Benefits of a Carbohydrate-Restricted Diet on Hepatic Steatosis in Humans.” *Cell Metabolism* 27 (3): 559–71.e5.

Matson, Vyara, Jessica Fessler, Riyue Bao, Tara Chongsuwat, Yuanyuan Zha, Maria-Luisa Alegre, Jason J. Luke, and Thomas F. Gajewski. 2018. “The Commensal Microbiome Is Associated with anti–PD-1 Efficacy in Metastatic Melanoma Patients.” *Science* 359 (6371): 104–8.

Morton, Angela M., Esen Sefik, Rabi Upadhyay, Ralph Weissleder, Christophe Benoist, and Diane Mathis. 2014. “Endoscopic Photoconversion Reveals Unexpectedly Broad Leukocyte Trafficking to and from the Gut.” *Proceedings of the National Academy of Sciences of the United States of America* 111 (18): 6696–6701.

Murray, Andrew J., Nicholas S. Knight, Mark A. Cole, Lowri E. Cochlin, Emma Carter, Kirill Tchabanenko, Tica Pichulik, et al. 2016. “Novel Ketone Diet Enhances Physical and Cognitive Performance.” *FASEB Journal: Official Publication of the Federation of American Societies for Experimental Biology* 30 (12): 4021–32.

Neal, Elizabeth G., Hannah Chaffe, Ruby H. Schwartz, Margaret S. Lawson, Nicole Edwards, Geogianna Fitzsimmons, Andrea Whitney, and J. Helen Cross. 2008. “The Ketogenic Diet for the Treatment of Childhood Epilepsy: A Randomised Controlled Trial.” *Lancet Neurology* 7 (6): 500–506.

Newman, John C., Anthony J. Covarrubias, Minghao Zhao, Xinxing Yu, Philipp Gut, Che-Ping Ng, Yu Huang, Saptarsi Haldar, and Eric Verdin. 2017. “Ketogenic Diet Reduces Midlife Mortality and Improves Memory in Aging Mice.” *Cell Metabolism* 26 (3): 547–

57.e8.

Newman, John C., and Eric Verdin. 2017. “β-Hydroxybutyrate: A Signaling Metabolite.” *Annual Review of Nutrition* 37 (August): 51–76.

Ni, Fen-Fen, Cheng-Rong Li, Jian-Xiang Liao, Guo-Bing Wang, Su-Fang Lin, Yu Xia, and Jia-Lun Wen. 2016. “The Effects of Ketogenic Diet on the Th17/Treg Cells Imbalance in Patients with Intractable Childhood Epilepsy.” *Seizure: The Journal of the British Epilepsy Association* 38 (May): 17–22.

Okonechnikov, Konstantin, Olga Golosova, Mikhail Fursov, and UGENE team. 2012. “Unipro UGENE: A Unified Bioinformatics Toolkit.” *Bioinformatics* 28 (8): 1166–67.

Olson, Christine A., Helen E. Vuong, Jessica M. Yano, Qingxing Y. Liang, David J. Nusbaum, and Elaine Y. Hsiao. 2018. “The Gut Microbiota Mediates the Anti-Seizure Effects of the Ketogenic Diet.” *Cell* 173 (7): 1728–41.e13.

Paradis, Emmanuel, Julien Claude, and Korbinian Strimmer. 2004. “APE: Analyses of Phylogenetics and Evolution in R Language.” *Bioinformatics* 20 (2): 289–90.

Pickard, Joseph M., Melody Y. Zeng, Roberta Caruso, and Gabriel Núñez. 2017. “Gut Microbiota: Role in Pathogen Colonization, Immune Responses, and Inflammatory Disease.” *Immunological Reviews* 279 (1): 70–89.

Pissios, Pavlos, Shangyu Hong, Adam Richard Kennedy, Deepthi Prasad, Fen-Fen Liu, and Eleftheria Maratos-Flier. 2013. “Methionine and Choline Regulate the Metabolic Phenotype of a Ketogenic Diet.” *Molecular Metabolism* 2 (3): 306–13.

Powell, Nick, Marjorie M. Walker, and Nicholas J. Talley. 2017. “The Mucosal Immune

System: Master Regulator of Bidirectional Gut-Brain Communications." *Nature Reviews. Gastroenterology & Hepatology* 14 (3): 143–59.

Price, Morgan N., Paramvir S. Dehal, and Adam P. Arkin. 2010. "FastTree 2--Approximately Maximum-Likelihood Trees for Large Alignments." *PloS One* 5 (3): e9490.

Puchalska, Patrycja, and Peter A. Crawford. 2017. "Multi-Dimensional Roles of Ketone Bodies in Fuel Metabolism, Signaling, and Therapeutics." *Cell Metabolism* 25 (2): 262–84.

Roberts, Megan N., Marita A. Wallace, Alexey A. Tomilov, Zeyu Zhou, George R. Marcotte, Dianna Tran, Gabriella Perez, et al. 2017. "A Ketogenic Diet Extends Longevity and Healthspan in Adult Mice." *Cell Metabolism* 26 (3): 539–46.e5.

Rooks, Michelle G., and Wendy S. Garrett. 2016. "Gut Microbiota, Metabolites and Host Immunity." *Nature Reviews. Immunology* 16 (6): 341–52.

Round, June L., S. Melanie Lee, Jennifer Li, Gloria Tran, Bana Jabri, Talal A. Chatila, and Sarkis K. Mazmanian. 2011. "The Toll-like Receptor 2 Pathway Establishes Colonization by a Commensal of the Human Microbiota." *Science* 332 (6032): 974–77.

Sainsbury, Emma, Nathalie V. Kizirian, Stephanie R. Partridge, Timothy Gill, Stephen Colagiuri, and Alice A. Gibson. 2018. "Effect of Dietary Carbohydrate Restriction on Glycemic Control in Adults with Diabetes: A Systematic Review and Meta-Analysis." *Diabetes Research and Clinical Practice* 139 (May): 239–52.

Sarafian, Magali H., Matthew R. Lewis, Alexandros Pechlivanis, Simon Ralphs, Mark J. W. McPhail, Vishal C. Patel, Marc-Emmanuel Dumas, Elaine Holmes, and Jeremy K.

Nicholson. 2015. “Bile Acid Profiling and Quantification in Biofluids Using Ultra-Performance Liquid Chromatography Tandem Mass Spectrometry.” *Analytical Chemistry* 87 (19): 9662–70.

Saslow, Laura R., Jennifer J. Daubenmier, Judith T. Moskowitz, Sarah Kim, Elizabeth J. Murphy, Stephen D. Phinney, Robert Ploutz-Snyder, et al. 2017. “Twelve-Month Outcomes of a Randomized Trial of a Moderate-Carbohydrate versus Very Low-Carbohydrate Diet in Overweight Adults with Type 2 Diabetes Mellitus or Prediabetes.” *Nutrition & Diabetes* 7 (12): 304.

Scher, Jose U., Andrew Sczesnak, Randy S. Longman, Nicola Segata, Carles Ubeda, Craig Bielski, Tim Rostron, et al. 2013. “Expansion of Intestinal Prevotella Copri Correlates with Enhanced Susceptibility to Arthritis.” *eLife* 2 (November): e01202.

Schugar, Rebecca C., Xiaojing Huang, Ashley R. Moll, Elizabeth M. Brunt, and Peter A. Crawford. 2013. “Role of Choline Deficiency in the Fatty Liver Phenotype of Mice Fed a Low Protein, Very Low Carbohydrate Ketogenic Diet.” *PloS One* 8 (8): e74806.

Segata, Nicola, Levi Waldron, Annalisa Ballarini, Vagheesh Narasimhan, Olivier Jousson, and Curtis Huttenhower. 2012. “Metagenomic Microbial Community Profiling Using Unique Clade-Specific Marker Genes.” *Nature Methods* 9 (8): 811–14.

Sharon, Gil, Nikki Jamie Cruz, Dae-Wook Kang, Michael J. Gandal, Bo Wang, Young-Mo Kim, Erika M. Zink, et al. 2019. “Human Gut Microbiota from Autism Spectrum Disorder Promote Behavioral Symptoms in Mice.” *Cell* 177 (6): 1600–1618.e17.

Silverman, Justin D., Alex D. Washburne, Sayan Mukherjee, and Lawrence A. David. 2017.

"A Phylogenetic Transform Enhances Analysis of Compositional Microbiota Data." *eLife* 6 (February). https://doi.org/10.7554/eLife.21887.

Sonnenburg, Justin L., Jian Xu, Douglas D. Leip, Chien-Huan Chen, Benjamin P. Westover, Jeremy Weatherford, Jeremy D. Buhler, and Jeffrey I. Gordon. 2005. "Glycan Foraging in Vivo by an Intestine-Adapted Bacterial Symbiont." *Science* 307 (5717): 1955–59.

Sprouffske, Kathleen, and Andreas Wagner. 2016. "Growthcurver: An R Package for Obtaining Interpretable Metrics from Microbial Growth Curves." *BMC Bioinformatics* 17 (April): 172.

Stubbs, Brianna J., Pete J. Cox, Rhys D. Evans, Peter Santer, Jack J. Miller, Olivia K. Faull, Snapper Magor-Elliott, Satoshi Hiyama, Matthew Stirling, and Kieran Clarke. 2017. "On the Metabolism of Exogenous Ketones in Humans." *Frontiers in Physiology* 8 (October): 848.

Tan, Tze Guan, Esen Sefik, Naama Geva-Zatorsky, Lindsay Kua, Debdut Naskar, Fei Teng, Lesley Pasman, et al. 2016. "Identifying Species of Symbiont Bacteria from the Human Gut That, Alone, Can Induce Intestinal Th17 Cells in Mice." *Proceedings of the National Academy of Sciences of the United States of America* 113 (50): E8141–50.

Thingholm, Louise B., Malte C. Rühlemann, Manja Koch, Brie Fuqua, Guido Laucke, Ruwen Boehm, Corinna Bang, et al. 2019. "Obese Individuals with and without Type 2 Diabetes Show Different Gut Microbial Functional Capacity and Composition." *Cell Host & Microbe* 26 (2): 252–64.e10.

Tognini, Paola, Mari Murakami, Yu Liu, Kristin L. Eckel-Mahan, John C. Newman, Eric

Verdin, Pierre Baldi, and Paolo Sassone-Corsi. 2017. “Distinct Circadian Signatures in Liver and Gut Clocks Revealed by Ketogenic Diet.” *Cell Metabolism* 26 (3): 523–38.e5.

Turnbaugh, Peter J., Fredrik Bäckhed, Lucinda Fulton, and Jeffrey I. Gordon. 2008. “Diet-Induced Obesity Is Linked to Marked but Reversible Alterations in the Mouse Distal Gut Microbiome.” *Cell Host & Microbe* 3 (4): 213–23.

Turnbaugh, Peter J., Ruth E. Ley, Michael A. Mahowald, Vincent Magrini, Elaine R. Mardis, and Jeffrey I. Gordon. 2006. “An Obesity-Associated Gut Microbiome with Increased Capacity for Energy Harvest.” *Nature* 444 (7122): 1027–31.

Turnbaugh, Peter J., Vanessa K. Ridaura, Jeremiah J. Faith, Federico E. Rey, Rob Knight, and Jeffrey I. Gordon. 2009. “The Effect of Diet on the Human Gut Microbiome: A Metagenomic Analysis in Humanized Gnotobiotic Mice.” *Science Translational Medicine* 1 (6): 6ra14.

Vandeputte, Doris, Gunter Kathagen, Kevin D’hoe, Sara Vieira-Silva, Mireia Valles-Colomer, João Sabino, Jun Wang, et al. 2017. “Quantitative Microbiome Profiling Links Gut Community Variation to Microbial Load.” *Nature* 551 (7681): 507–11.

Veech, Richard L., Patrick C. Bradshaw, Kieran Clarke, William Curtis, Robert Pawlosky, and M. Todd King. 2017. “Ketone Bodies Mimic the Life Span Extending Properties of Caloric Restriction.” *IUBMB Life* 69 (5): 305–14.

Volek, Jeff S., Stephen D. Phinney, Cassandra E. Forsythe, Erin E. Quann, Richard J. Wood, Michael J. Puglisi, William J. Kraemer, Doug M. Bibus, Maria Luz Fernandez, and Richard D. Feinman. 2009. “Carbohydrate Restriction Has a More Favorable Impact on the

Metabolic Syndrome than a Low Fat Diet." *Lipids* 44 (4): 297–309.

Wang, Qiong, George M. Garrity, James M. Tiedje, and James R. Cole. 2007. "Naive Bayesian Classifier for Rapid Assignment of rRNA Sequences into the New Bacterial Taxonomy." *Applied and Environmental Microbiology* 73 (16): 5261–67.

Winer, Daniel A., Helen Luck, Sue Tsai, and Shawn Winer. 2016. "The Intestinal Immune System in Obesity and Insulin Resistance." *Cell Metabolism* 23 (3): 413–26.

Publishing Agreement

It is the policy of the University to encourage the distribution of all theses, dissertations, and manuscripts. Copies of all UCSF theses, dissertations, and manuscripts will be routed to the library via the Graduate Division. The library will make all theses, dissertations, and manuscripts accessible to the public and will preserve these to the best of their abilities, in perpetuity.

Please sign the following statement:

I hereby grant permission to the Graduate Division of the University of California, San Francisco to release copies of my thesis, dissertation, or manuscript to the Campus Library to provide access and preservation, in whole or in part, in perpetuity.

DocuSigned by:
CAD0126AFACC42E...

Author Signature

12/4/2019

Date